Alma Mater Studiorum – Università di Bologna

DOTTORATO DI RICERCA IN

SCIENZE BIOTECNOLOGICHE, BIOCOMPUTAZIONALI, FARMACEUTICHE E FARMACOLOGICHE

Ciclo XXXIII

Settore Concorsuale: 03/D1

Settore Scientifico Disciplinare: CHIM/08

BIOLOGICAL ANALYSIS OF THE IN-VITRO EFFECTS OF HOMOLOGOUS RECOMBINATION INHIBITION AND ITS USE IN CANCER TREATMENT THROUGH SYNTHETIC LETHALITY

Presentata da: Andrea Balboni

Coordinatore Dottorato
Prof.ssa Maria Laura Bolognesi

Supervisore
Prof. Andrea Cavalli

Co-Supervisore
Prof.ssa Giuseppina di Stefano

Esame finale anno 2021

TABLE OF CONTENTS:

ABSTRACT

Synthetic lethality represents an anticancer strategy that targets tumor specific gene defects. One of the most studied application is the use of PARP inhibitors (e.g., olaparib) in BRCA1/2-less cancer cells. In BRCA2-defective tumors, olaparib (OLA) inhibits DNA single-strand break repair, while BRCA2 mutations hamper homologous recombination (HR) repair. The simultaneous impairment of those pathways leads BRCA-less cells to death by synthetic lethality.

The projects described in this thesis were aimed at extending the use of OLA in cancer cells that do not carry a mutation in BRCA2 by combining this drug with compounds that could mimic a BRCA-less environment via HR inhibition. Contrary to the conventional use of OLA in cancer treatment, this "fully small-molecule induced synthetic lethality" could be applied to a higher variety of cancer types.

We demonstrated the effectiveness of our "fully small-molecule induced synthetic lethality" by using two different approaches.

In the direct approach (**Project A**), we identified a series of neo-synthesized compounds (named RAD51-BRCA2 disruptors) that mimic BRCA2 mutations by disrupting the RAD51-BRCA2 interaction and thus the HR pathway. Compound ARN 24089 showed the most promising results in our experiments. ARN 24089 inhibited HR in human pancreatic adenocarcinoma cell line and triggered synthetic lethality by synergizing with OLA. Interestingly, the observed synthetic lethality was triggered by tackling two biochemically different mechanisms: enzyme inhibition (PARP) and protein-protein disruption (RAD51-BRCA2). This highlights how complex and diverse mechanisms of action can synergistically contribute to the same physiological and, in turn, pharmacological activity.

In the indirect approach (**Project B**), we inhibited HR by interfering with the cellular metabolism through inhibition of LDH activity. Various studies hint a possible connection between the activity of this enzyme and the efficiency of DNA repair pathways. The obtained data suggest an LDH-mediated control on HR that can be exerted by regulating either the energy supply needed to this repair mechanism or the expression level of genes involved in DNA repair. LDH inhibition also succeeded in increasing the efficiency of OLA in BRCA-proficient cell lines. Although preliminary, these results highlight a complex relationship between metabolic reactions and the control of DNA integrity.

Both the described projects proved the possibility to widen the use of OLA in BRCA-competent and OLA-resistant cancers, making this "fully small-molecule-induced synthetic lethality" an innovative approach to unmet oncological needs.

1. ABBREVIATIONS

- **4EBP1:** 4E-Binding Protein 1
- **ADP:** Adenosine DiPhosphate
- **AIF:** Apoptosis Inducing Factor
- **ASCO:** American Society of Clinical Oncology
- **ATM:** Ataxia-Telangiectasia Mutated serine/threonine kinase
- **ATP:** Adenosine TriPhosphate
- **BAX:** Bcl-2-associated X protein
- **BCL-2:** B-cell lymphoma 2 protein
- **BCR/ABL:** Breakpoint Cluster Region/ Abelson protein
- **BRCA1 / 2:** Breast Cancer-Associated 1/2
- **BxPC3:** Human primary pancreatic adenocarcinoma
- **CAFs:** Cancer Associated Fibroblasts
- **Capan-1:** Human primary pancreatic adenocarcinoma, devoid of BRCA2 activity
- **CDC6:** Cell Division Control protein 6
- **Cdc25C:** Cell division cycle 25C
- **CML:** Chronic Myeloid Leukemia
- **CPL:** Cisplatin
- **DAPI:** 4′,6-diamidino-2-phenylindole
- **DBD:** DNA-Binding Domain

- **DDR:** DNA-damage repair
- **del[5q]:** chromosome 5q deletion
- **DNA:** DeoxyriboNucleic Acid
- **DNA-PK:** DNA-dependent Protein Kinase
- **DNA-PKcs:** DNA-dependent Protein Kinase catalytic subunit
- **DSBs:** Double-Strand Breaks
- **EJ:** alternate End Joining
- **FDA:** Food and Drug Administration
- **GATA2:** GATA binding protein 2
- **gBRCAm:** germline BRCA mutated
- **GLUT1/3:** GLUcose Transformer 1/3
- **H2B:** Histone 2B
- **HAT:** Histone acetyltransferase
- **HDAC:** Histone deacetylase
- **HER2:** Human Epidermal growth factor Receptor 2
- **HIF-1:** Hypoxia-Induced Factor-1
- **HK-2:** Human Kidney-2
- **hnRNPA0:** Heterogeneous Nuclear Ribonucleoprotein A0
- **HR:** Homologous Recombination
- **IL-8/17A:** InterLeukin-8/17A

- **LDH-A/B:** Lactate DeHydrogenase-subunit A/B
- **mCRPC:** metastatic Castration-Resistant Prostate Cancer
- **MDS:** MyeloDysplastic Syndrome
- **MAPKAPK2 (MK2):** MAPK Activated Protein Kinase 2
- **mTOR:** mechanistic Target Of Rapamycin
- **MYC:** myc proto-oncogene protein
- **NAD:** Nicotinamide Adenine Dinucleotide
- **NHEJ:** Non-Homologous DNA End Joining
- **NSCLC:** Non-Small-Cell Lung Cancer
- **OLA:** Olaparib
- **OXA:** Oxamate
- **PAK2:** P21 Activated Kinase 2
- **pARG:** Poly(ADP-Ribose) Glycohydrolase
- **PARP:** Poly [ADP-ribose] polymerase
- **PI:** Propidium iodide
- **PP2Aca:** Protein Phosphatase 2A catalytic subunit a
- **RAD51:** DNA Recombinase and DNA Repair Protein
- **ROS:** Reactive Oxygen Species
- **RPA:** Replication Protein A
- **RPS14:** Ribosomal Protein S14

- **SGK2:** Serum/Glucocorticoid regulated Kinase 2
- **SSBs:** Single-Strand Breaks
- **STI_{571}:** protein-tyrosine kinase inhibitor
- **SW620:** Human Caucasian colon adenocarcinoma
- **TCA cycle:** TriCarboxylic Acid cycle
- **VEGF:** Vascular Endothelial Growth Factor
- **XRCC4:** X-Ray Repair Cross Complementing 4

2. INTRODUCTION

2.1 SYNTHETIC LETHALITY

2.1.1 Cancer overview

Cancer is globally the second leading cause of death, and is responsible for an estimated 9.6 million deaths in 2018. The name Cancer refers to a class of diseases in which abnormal cells divide without control and can invade nearby tissues. Cancer cells can also spread to other parts of the body through the blood and lymph systems. There are several main types of cancer. Carcinoma is a cancer that originates from epithelial tissues. Sarcoma is a cancer that begins in bone, cartilage, fat, muscle, blood vessels, or other connective or supportive tissue. Leukemia is a cancer that starts in blood-forming tissue, such as the bone marrow, and causes large numbers of abnormal blood cells to be produced and enter the blood. Lymphoma and multiple myeloma are cancers that begin in the cells of the immune system [1].
In 2018 the most common causes of cancer death, worldwide, were Lung cancer (1.76 million deaths), Colorectal (862.000 deaths), Stomach (783.000 deaths), Liver (782.000 deaths) and Breast (627.000 deaths). Every cancer type requires a specific treatment regimen that encompasses one or more modalities such as surgery, radiotherapy, and chemotherapy [2].

2.1.2 Use of inhibiting strategies for Cancer treatments

Even though some cancers now have a higher survivability rate, there is still much to do and the discovery of new anticancer therapies is a critical point in the world of clinical research; in the past decades, researchers all over the world focused on developing new therapies centered on target genes or proteins that are critical for the cancer cells.
Some therapies revolve around the activities of inhibiting molecules such as STI_{571}, a tyrosine kinase inhibitor used in the treatment of Chronic Myeloid Leukemia (CML): CML is a malignant clonal disorder of hematopoietic stem cells that results in increases in myeloid cells and marked myeloid hyperplasia in the bone marrow [3]. CML is characterized by a balanced translocation between chromosome 9 and 22 that leads to the formation of BCR/ABL, a chimeric protein characterized by an unregulated tyrosine kinase activity [4]. Since the activity of BRC/ABL is essential for CML cells, by administering them a tyrosine kinase inhibitor like STI_{571} a cytogenetic remission can be observed that can lead to an increase in cancer cell death and in an increase in the patient survival [5].
Against other types of cancers, the therapies involve the use of monoclonal antibodies; a perfect example is the use of Bevacizumab for the treatment of Renal Cell Carcinoma. This carcinoma presents an increase in the transcription of several hypoxia-inducible genes, one of them being VEGF (Vascular Endothelial Growth Factor) a potent proangiogenic molecule

that inhibits dendritic cell maturation and tumor cell apoptosis and stimulates tumor angiogenesis [6]. Administering interferon Alfa along with Bevacizumab, a humanized monoclonal antibody that inhibits VEGF, produces significant and clinically meaningful improvements in progression-free survival and overall response rates. These findings indicate that the bevacizumab/interferon Alfa association is a promising option for first-line treatment for patients with metastatic renal cell carcinoma. [7]
Those targeted therapies, however, have some limitations since it is not always possible to target a protein or a gene that plays a central role in a cellular pathway. Side effects arising by on- and off-targets are always an issue because the inhibitors could target also the healthy cells. In order to perfect these precision therapies, many researchers have started to focus their attention on "synthetic lethality".

2.1.3 Synthetic lethality

The concept of synthetic lethality originates from studies in drosophila model systems in which a combination of mutations in two or more separate genes leads to cell death, while the single mutated genes do not affect the viability of the cell [8] [**Figure 2.1**]. These tumor-specific genetic defects lead to the use of targeted agents that induce the death of tumor cells while sparing normal cells. Oncogenic drivers such as mutated *KRAS* and *MYC* can be targeted with synthetic-lethality approaches.
Oncogenic mutations in *RAS* genes are very common in human cancer and its removal from tumor cell lines resulted in reversal of cell transformation [9]. However, a selective inhibition of that protein using drugs has so far proven to be impossible. Carrying out a large-scale loss-of-function screen, researchers discovered that *RAS* mutated cell lines were highly dependent on the transcription factor GATA2 and the DNA replication initiation regulator CDC6. These same cells showed synthetic lethality with topoisomerase inhibition. Combination targeting of these functions caused improved killing of *KRAS* mutant cells relative to wild-type cells. [10]
MYC is also one of the most commonly deregulated oncogenes in human cancer, yet therapies directly targeting *MYC* hyper-activation are not presently available in the clinic. The evolutionarily conserved function of *MYC* in modulating protein synthesis control is critical for its oncogenic program [11]. Therefore, inhibiting enhanced protein synthesis represents a highly relevant strategy for the treatment of *MYC*-dependent human cancers. Researchers found, using a pharmacogenetic approach, that mTOR-dependent phosphorylation of 4EBP1 (a regulator of protein synthesis control) is required for cancer cell survival in *MYC*-dependent tumor initiation and maintenance. They also discovered that a clinical mTOR active site inhibitor, which is capable of blocking mTOR-dependent 4EBP1 phosphorylation, has remarkable therapeutic efficacy in *MYC*-driven hematological cancers [12].

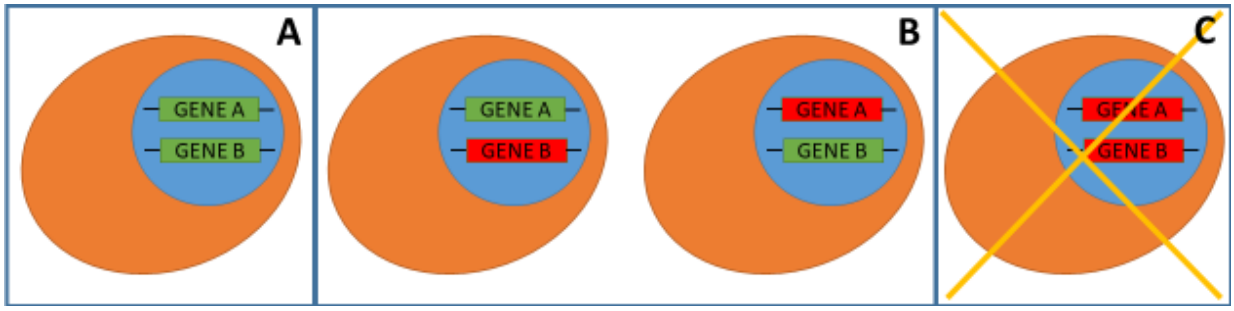

Figure 2.1. *(A) Gene A and Gene B are both without mutations and the cell is alive. (B) One of the genes is mutated while the other is still without mutations; this situation does not impair cellular viability. (C) Both genes are mutated, leading to cell death through synthetic lethality.*

Synthetic lethality can also be applied in patients suffering from Myelodysplastic Syndrome (MDS) with a chromosome 5q deletion (del[5q]), which is the most common chromosomal abnormality detected in MDS with an overall case prevalence of 10%–15%. This deletion leads to haploinsufficiency of genes encoded within the commonly deleted region at 5q31 to 5q32, including the ribosomal subunit 14 gene (*RPS14*) [13].

In December 2005, the United States Food and Drug Administration (FDA) approved lenalidomide (Revlimid; Celgene Corporation) for the treatment of transfusion-dependent, lower-risk patients with del[5q] MDS. Suppression of del[5q] clones by lenalidomide arises mainly from inhibition of two phosphatases that are co-regulators of the G2–M checkpoint: cell division cycle 25 homologue C (CDC25C) and protein phosphatase 2A (PP2A) catalytic subunit alpha (PP2Aca). Allelic haploinsufficiency of both phosphatases leads to enhanced sensitivity to lenalidomide; this portrays the principle of synthetic lethality in practice, whereas overexpression of PP2A is associated with secondary resistance to this agent [14].

Synthetic lethality can also be useful in targeting tumors with a mutated *TP53* gene. It is difficult to target mutant p53 protein or restore functional p53 activity directly in a manner that translates readily into a clinical benefit. For this reason, identification of genes that show synthetic lethality with it is an area of active investigation. For instance, the stress-activated p38 mitogen-activated protein kinase MAPKAP kinase 2 (MK2) appears to be essential for survival of p53-deficient non–small-cell lung cancer (NSCLC) cells in response to chemotherapy. A study showed that, in cells lacking functional p53, MK2 could induce a cell-cycle checkpoint after genotoxic stress [15]. This occurs through modulation of the RNA-binding protein hnRNPA0, promoting the association of hnRNPA0 with the cyclin-dependent kinase inhibitor GADD45A, and up-regulation of microRNA *miR-34c*, which can indirectly promote S-phase arrest. Deficiency of MK2 in autochthonous p53-deficient murine NSCLC models leads to augmented cisplatin sensitization.

Furthermore, ATM suppression in p53-deficient tumors can directly sensitize tumors to chemotherapy; in contrast, ATM suppression in models of p53-proficient tumors can induce chemoresistance [16]. In addition, a study in models of cervical cancer has shown that depletion of either SGK2 or PAK3, in combination with loss of p53 activity, inhibits cell

survival by inducing autophagy (with SGK2 depletion) or apoptosis (with PAK3 depletion). Therefore, potential approaches exist for targeting these proteins in tumors with *Tp53* mutations [17].

Our project revolves around another synthetic lethality gene pair: BRCA2, involved in double strand repair, and PARP, involved in single strand repair. Several studies revealed that dysfunction of BRCA1 and BRCA2 dramatically sensitized cells to poly (adenosine diphosphate [ADP]–ribose) polymerase (PARP) inhibitors because of associated defective homologous recombination and the inability to mount efficient DNA repair [18].

2.2 PARP INHIBITORS

2.2.1 Poly (ADP-ribose) Polymerase

Poly (ADP-ribose) polymerase (PARP) is responsible for post-translational modification of proteins in response to numerous endogenous and environmental genotoxic agents. PARP and poly (ADP-ribosyl)ation are involved in the regulation of many cellular processes such as DNA repair, cell death, chromatin functions and genomic stability. Activation of PARP is one of the early DNA damage responses, among other DNA sensing molecules, such as DNA-PK, ATM and p53 [19].

PARP presents two distinct regions: an amino-terminal DNA-binding domain with two zinc-fingers (28-30 residues), essential for binding to DNA breaks, and a carboxy-terminal catalytic domain. Experimental data showed that PARP tends to preferentially bind at DNA breaks, covering 7-8 residues at each side of the breaks [20]. The spacing between the amino acids in the zinc-fingers is unusual, but similar arrangements have been observed in the amino-terminal region of human DNA ligase III and in the carboxy-terminal region of DNA polymerase ε; this structure is believed to be fundamental for preferring the binding at DNA breaks sites [21-22].

The catalytic domain shows homologies to NAD-binding sites observed in other enzymes; this domain requires PARP to be bound to the DNA in order to catalyze an efficient polymer synthesis. Interestingly, the strand interruptions regularly occurring during DNA replication do not trigger Poly (ADP-ribosyl)ation, probably because the replisomes that protect the termini of Okazaki fragments prevent the access of PARP and other enzymes that are not directly involved in the replication process [23].

The process of Poly (ADP-ribosyl)ation is catalyzed primarily by poly(ADP-ribose) polymerase-1 (PARP1), which is the most abundant of the 18 different PARP isoforms and accounts for more than 90% of the catalytic activity of PARP in the cell nucleus. Upon detection of a DNA strand break, PARP1 binds to the DNA, cleaves nicotinamide adenine dinucleotide (NAD) between nicotinamide and ADP-ribose and then modifies the DNA nuclear acceptor proteins (PARP included) by formation of a bond between the proteins and the ADP-ribose residue. This generates ribosyl–ribosyl linkages that act as a signal for other

DNA-repairing enzymes and DNA base repair [24]. Several Glu residues, situated between the DNA binding domain and the Catalytic domain, serve as anchor points for Poly (ADP-ribose) polymer synthesis: these polymers can form branches and become up to several hundred residues long. After the DNA has been repaired, these branches are slowly degraded by the Poly (ADP-ribose) glycohydrolase enzyme (pARG), liberating free ADP-ribose monomers [25].

Studies have shown that the auto-modified PARP differs from the original enzyme in being unable to bind to DNA. This can be explained by the fact that ADP-ribose is strongly negatively charged and charge repulsion between the branches and the DNA leads the release of the auto-modified enzyme. This detachment shuts down ulterior branch synthesis, which are then removed by the action of pARG, and this grants PARP the ability to shuttle on and off damaged DNA. Since pARG acts slowly it creates a useful window in which DNA repair can occur before PARP reattaches itself to the lesion [26].

Whereas activation of PARP by mild genotoxic stimuli may facilitate DNA repair and cell survival, irreparable DNA damage triggers apoptotic or necrotic cell death. In apoptosis, early PARP activation may assist the apoptotic cascade by stabilizing p53, by mediating the translocation of apoptosis inducing factor (AIF) from the mitochondria to the nucleus or by inhibiting early activation of DNases. In most severe oxidative stress situations, excessive DNA damage causes over activation of PARP, which incapacitates the apoptotic machinery (via depletion of NAD reserves) and switches the mode of cell death from apoptosis to necrosis [27].

2.2.2 Olaparib

Poly (ADP-ribose) polymerase (PARP) inhibitors have been studied as potential cancer therapeutics in breast and ovarian cancers. PARP inhibitors have several documented mechanisms of action, including the inhibition of base excision repair (via blockade of enzymatic function) as well as trapping of PARP upon the DNA [28]. Tumors in which there is an apparent defect in homologous DNA repair (and thus defect in repair of double-stranded breaks) seem to be susceptible to PARP inhibitor therapy. These include tumors associated with germline or somatic mutations in BRCA1 and BRCA2 (BRCA1/2) [29] [**Figure 2.2**].

PARP inhibitors target and bind the catalytic domain of the protein, preventing the formation of the ADP-ribose branches and the subsequent detachment of the protein from the damaged area. By blocking PARP on the DNA, these small molecules can interfere with the whole repair mechanism.

In 2011 encouraging results of Phase II clinical trials involving a PARP inhibitor called Iniparib were published in peer-reviewed journals. In one of the studies, which included patients with triple-negative breast cancer, the inclusion of Iniparib to chemotherapy improved the clinical benefit and survival of patients without significantly increased toxic effects. The addition of Iniparib to chemotherapeutic drugs improved the rate of clinical

benefit from 34% to 56% and the rate of overall response from 32% to 52%. The addition of Iniparib also prolonged the median progression-free survival from 3.6 months to 5.9 months and the median overall survival from 7.7 months to 12.3 months. [30].

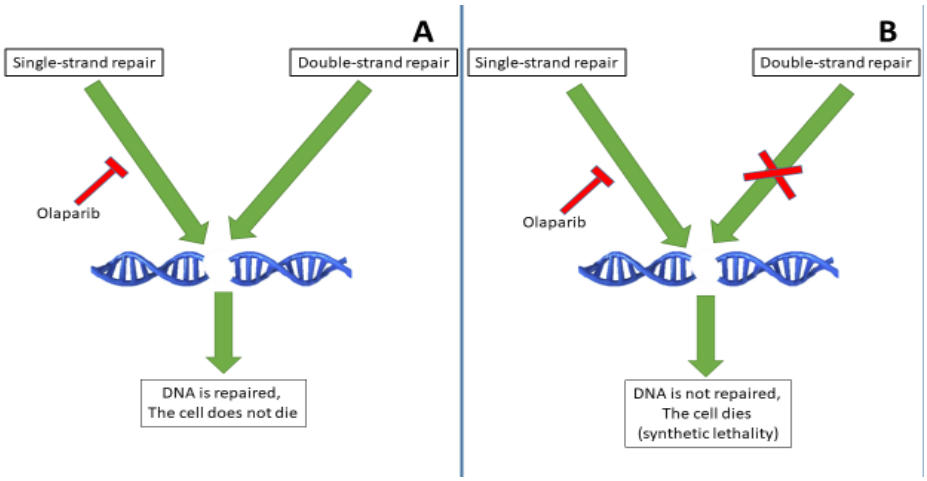

Figure 2.2. *(A) PARP inhibitor prevent PARP from being located on SSB. In normal cells SSB are converted to DSB and repaired through homologous recombination. (B) In BRCA-mutated cells DSB is not repaired effectively, leading to cell death.*

One of the most famous PARP inhibitors available is Olaparib (Lynparza™). Olaparib (OLA) is an oral, small molecule, poly (ADP-ribose) polymerase inhibitor that has been approved from FDA for the treatment of BRCA mutation-positive ovarian cancer [**Figure 2.3**].

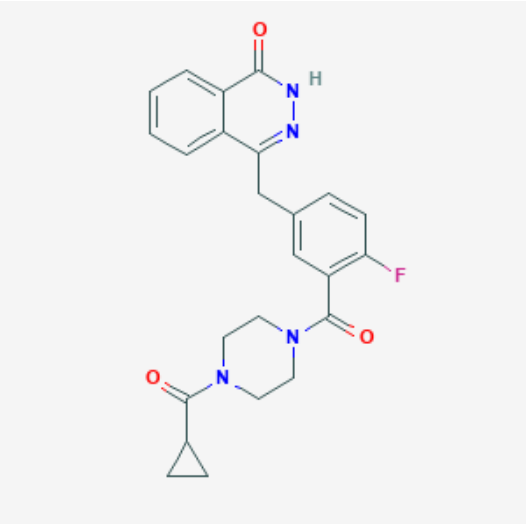

Figure 2.3. *Chemical structure of Olaparib [PubChem; 23725625]*

This molecule acts on PARP-1, PARP-2 and PARP-3 and inhibits them, preventing the formation of the ADP-ribose branches thus increasing the formation of PARP-DNA complexes, disrupting cellular homeostasis and causing cell death [31].

OLA has been indicated for the treatment of different types of cancers [32]:

- Ovarian Cancer: for the maintenance treatment of adult patients with deleterious or suspected deleterious germline or somatic BRCA-mutated advanced cancer who are in complete or partial response to first-line platinum-based chemotherapy. OLA is used also for the treatment of adult patients with deleterious or suspected deleterious germline BRCA mutated (gBRCAm) advanced ovarian cancer who have been treated with three or more prior lines of chemotherapy.
- Breast Cancer: for the treatment of adult patients with deleterious or suspected deleterious gBRCAm, HER2 negative metastatic breast cancer who have been treated with chemotherapy in the neo-adjuvant, adjuvant or metastatic setting.
- Pancreatic Cancer: for the maintenance treatment of adult patients with deleterious or suspected deleterious gBRCAm metastatic pancreatic adenocarcinoma whose disease has not progressed on at least 16 weeks of a first-line platinum-based chemotherapy regimen.
- Prostate Cancer: for the treatment of adult patients with deleterious or suspected deleterious germline or somatic homologous recombination repair (HRR) gene-mutated metastatic castration-resistant prostate cancer (mCRPC) who have progressed following prior treatment with enzalutamide or abiraterone.

OLA, similarly to other PARP inhibitors, is extremely efficient in tumors with compromised homologous recombination (HR) activity but has low or no effect on tumors where those specific alterations are missing. The aim of our project is to enhance the effect of OLA in BRCA-proficient tumors by recreating a BRCA-less environment in our cell lines through compounds that could impair the efficiency of the HR mechanism [**Figure 2.4**].

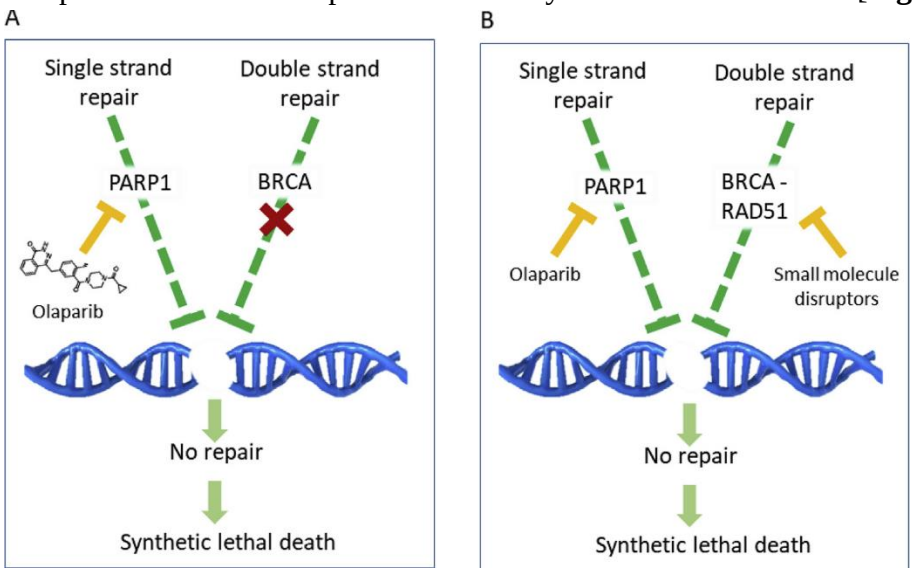

Figure 2.4. *(A) OLA inhibits PARP activity in a BRCA-deficient cell, leading to death by synthetic lethality. (B) OLA administered in a BRCA-proficient cell in association with a small molecule that impairs homologous recombination.*

2.3 DOUBLE STRAND DAMAGE REPAIR MECHANISMS

2.3.1 Double-strand breaks overview

Double-strand DNA breaks (DSBs) are common events in eukaryotic cells. There are an estimated ten DSBs per day per cell, based on metaphase chromosome and chromatid breaks in early passage primary human or mouse fibroblasts [33]. Major pathologic causes of double-strand breaks in wild type cells are caused by replication across a nick, giving rise to chromatid breaks during S phase. Reactive Oxygen Species (ROS) [34], Ionizing Radiations [35] and inadvertent action by nuclear enzymes on DNA (e.g., Topoisomerase activity) [36] can cause DSBs as well.

Cells use two major pathways for repairing DSBs: homologous recombination (HR) and non-homologous DNA end joining (NHEJ). NHEJ is the most common pathway used by cells for DSBs repair, while HR is mainly used during S-phase and G2-phase [**Figure 2.5**].

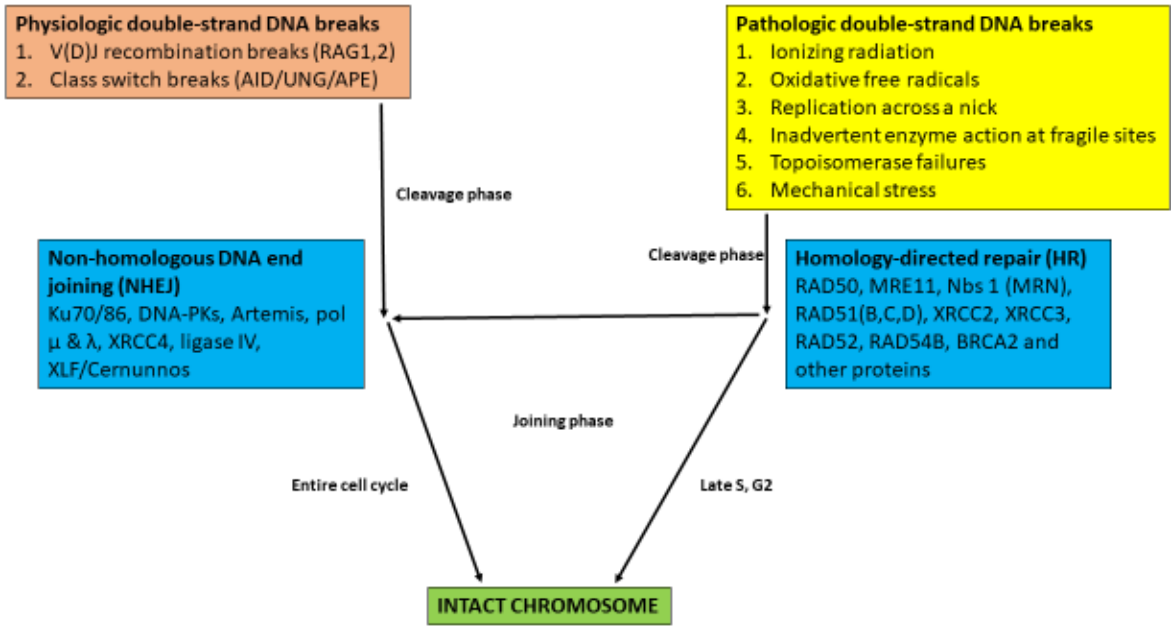

Figure 2.5. *Physiologic and pathologic causes of double-strand breaks in mammalian somatic cells are listed at the top. During S and G2 of the cell cycle, homology-directed repair is common because the two sister chromatids are in close proximity, providing a nearby homology donor. At any time in the cell cycle, double-strand breaks can be repaired by non-homologous DNA end joining (NHEJ). Proteins involved in the repair pathways are also listed.*

It is not fully clear how the pathways are selected, but it might be correlated to the distance between the damaged sequence and the homologous one. During S and G2 the sister chromatids are closer, thus HR is more likely to happen, while outside of those phases NHEJ is the only option [37]. Moreover, a hypothetical HR mechanism that could operate even on

distant homologous sequences could lead to chromosomal abnormalities through random recombination of repeated DNA sequences that are present all across the genome [38].

2.3.2 Non-homologous End Joining Repair

NHEJ is distinctive for the flexibility of the nuclease, polymerase, and ligase activities that are used. This flexibility permits NHEJ to function on the wide range of possible substrate configurations that can arise when double-strand breaks occur. When NHEJ takes place, the first protein that binds DNA is the KU heterodimer (KU70/KU80), thanks to its abundance in the nucleus and its high affinity for duplex DNA ends [39]. The KU-DNA complex serve as a node at which NHEJ's nucleases, polymerases and ligases can dock: this recruitment is very flexible and each protein can dock at any order. Other proteins involved in NHEJ are the nuclease complex Artemis-DNA PKcs (DNA-dependent Protein Kinase Catalytic Subunit), the two polymerases μ and λ and the ligases XRCC4 and DNA ligase IV [40].
The complex Artemis-DNA PKcs, upon coming into contact with the KU-DNA complex, phosphorylate themselves and start their endonuclease activity at the overhangs, but also at other single/double strand structures such as DNA hairpins [41].
Upon fortuitous pairing of the overhangs, the two polymerases are recruited and start to resynthesize the missing parts of the double strand filament; during the synthesis some template slippage could occur, which would lead to the formation of direct repeats. The evolutionary advantage of this becomes clear when considering a DSB in which there is no terminal microhomology between the two DNA ends. Random addition has the benefit of potentially generating one or two nucleotides of terminal microhomology, permitting more efficient annealing of the ends and thereby facilitating NHEJ [42].
Lastly, the ligases are recruited in order to complete the repair process and the XRCC4-DNA ligase IV complex shows a remarkable degree of flexibility. First, XRCC4-DNA ligase IV can ligate one strand independent of the other strand. Second, XRCC4-DNA ligase IV can ligate across gaps of even several nucleotides. Third, when KU is present, XRCC4-DNA ligase IV can ligate some incompatible DNA ends that have short overhangs. All of these aspects of the flexibility contribute to the range of DNA end configurations that XRCC4-DNA ligase IV can handle in its challenging role as the only ligase optimally suited for the repair of DSBs [43].
The NHEJ complex acts on both edges of the DNA damaged area and thanks to the high versatility of its pathway can manage to restore its integrity. However, since this process does not utilize a homologous sequence, some bases can be lost during the repair process and can lead to the accumulation of randomly located mutations over time in the genome of each somatic cell of an organism. [40].

2.3.3 Homologous recombination

HR provides high fidelity, template-dependent repair or tolerance of complex DNA damages including DNA gaps, DNA double-stranded breaks (DSBs), and DNA interstrand crosslinks (ICLs). In addition to its role in preserving the genome, HR plays a prominent role in faithfully duplicating the genome by providing critical support for DNA replication and telomere maintenance [44].

The central reaction of HR is homology search and DNA strand invasion by the RAD51-ssDNA filament, positioning the invading 3′-end on a template duplex DNA to initiate repair synthesis. In the nuclear environment the heterotrimeric ssDNA-binding protein RPA, which displays higher affinity and specificity for ssDNA than Rad51, initially binds ssDNA. Hence, in vivo RAD51 must assemble to form the presynaptic filament on RPA-coated ssDNA [45]. RPA inhibits nucleation of the RAD51 filament on ssDNA, but stimulates recombination by eliminating secondary structure in ssDNA and by binding to the displaced strand of the D-loop [46].

The tumor suppressor BRCA2 is a mediator of the core mechanism of homologous recombination. Heterozygous mutations in BRCA2 predispose to breast, ovarian as well as other tumor types. Bi-allelic loss of BRCA2 function causes Fanconi Anemia, a rare genetic disease resulting in impaired response to DNA damage [47]. BRCA2 contains eight conserved sequence motifs called BRC repeats, which are the primary RAD51 binding sites [48].

After the RAD51- BRCA2 complex is formed, RAD51 coats single-stranded DNA substrates to form a helical nucleoprotein filament, which can invade duplex DNA, and pair with homologous nucleotides to initiate the strand exchange reactions that culminate in genetic recombination. The interaction between BRCA2 and RAD51 is critical for the biological functions of both molecules and for the whole HR mechanism [**Figure 2.6**].

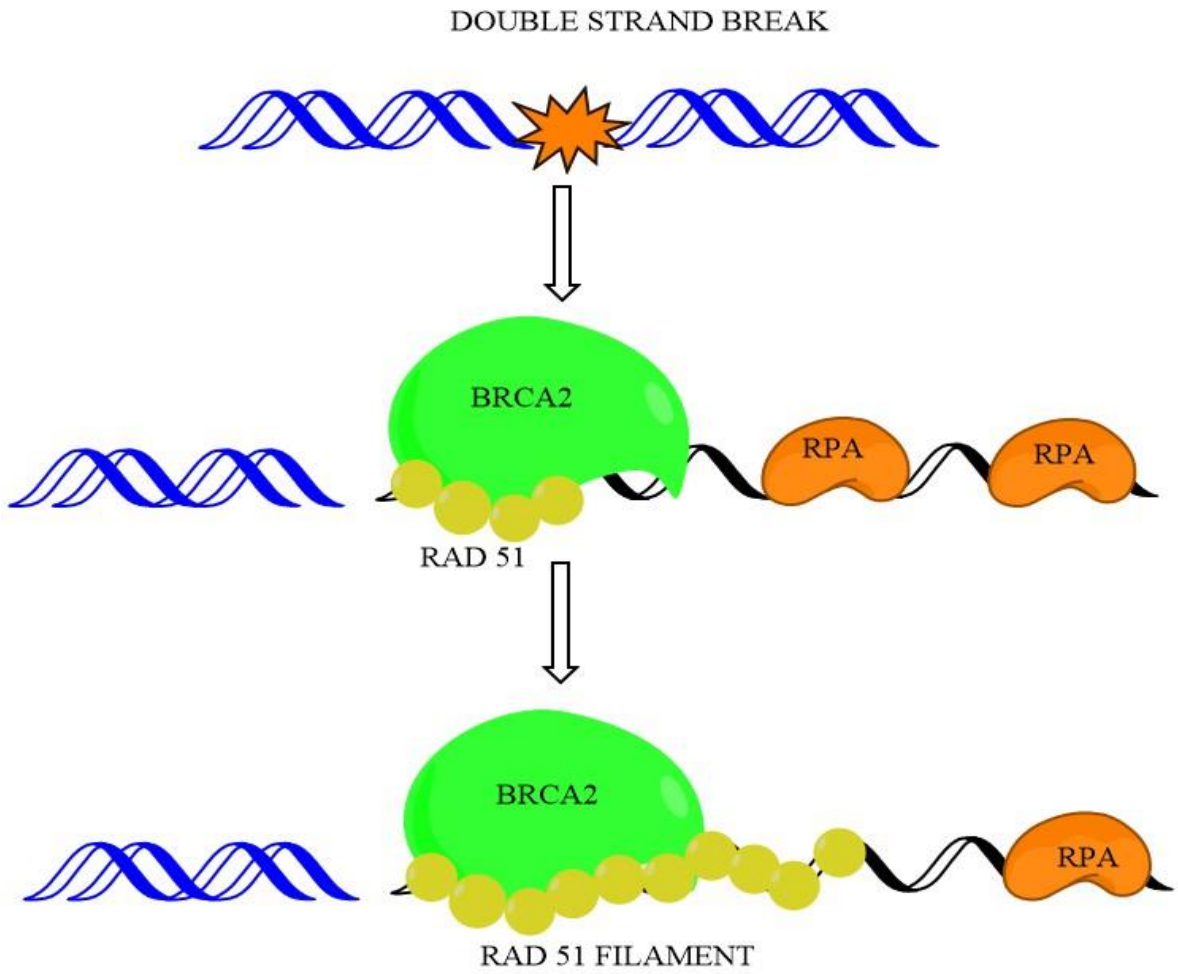

Figure 2.6. *After DNA is damaged, BRCA2 binds RAD51 with BRC 1-4, binds to ssDNA and recruits other RAD51 units. RAD51 localizes to the damaged filament by interacting with BRC 5-8, starts to form a RAD51 filament and displaces RPA in order to begin the strand invasion and the subsequently the repair of DNA.*

2.4 PROJECT A: INHIBITION OF HOMOLOGOUS RECOMBINATION ACTIVITY THROUGH THE USE OF RAD51-BRCA2 DISRUPTORS

2.4.1 BRCA2 structure

BRCA2 is a 3418-aminoacid long protein that is highly expressed during meiosis and localizes to the nucleus during the S phase. Crystallographic studies revealed that BRCA2 possesses both a DNA-binding domain (DBD), with unique structural features for binding ssDNA and dsDNA [49], and eight conserved sequence motifs—the BRC repeats—of about 30 amino acids each positioned between residues 990 and 2100 (in human BRCA2). Although the overall sequence similarity among BRCA2 orthologues is limited, the BRC repeats in different species are well conserved, suggesting that they are essential to the biological function of BRCA2 which is the interaction with Rad51 [50].

When expressed in vitro, six of the eight BRC repeats in BRCA2 can interact directly with recombinant RAD51. BRC3 and BRC4 encoded in human BRCA2 are particularly efficient at RAD51 binding, whereas BRC5 and BRC6 are not [51].
The binding of BRC4 with RAD51 is maintained by a series of hydrophilic and hydrophobic interactions conferred by a hairpin structure and a short linker that binds RAD51 in two different loci: the N-terminal domain and the nucleotide-binding core. The BRC4 sequence mimics that of RAD51's oligomerization motifs thus preventing its incorporation into RAD51 nucleoprotein filaments [52].
The presence of both the BRC repeats and the DBD on BRCA2 indicates that the protein can bind both RAD51 and the DNA and can deliver RAD51 to the sites of DNA breaks. A study revealed the existence of two categories of BRC repeats that display unique functional characteristics. One group, comprising BRC1, -2, -3, and -4, binds to free RAD51 with high affinity and reduces its ATPase activity. The second group, comprising BRC5, -6, -7, and -8, binds to free RAD51 with low affinity but binds to the RAD51-ssDNA filament with high affinity and does not reduce its ATPase activity. Thus, through different mechanisms, both types of BRC repeats bind to and stabilize the RAD51 nucleoprotein filament on ssDNA. These two groups of BRC repeats have differentially evolved to ensure efficient formation of a nascent RAD51 filament on ssDNA by promoting its nucleation and growth, respectively [53].

2.4.2 RAD51 structure

The RAD51 protein is the eukaryotic homolog of the prokaryotic RecA, and is the central recombinase in eukaryotes [54]. RAD51-mediated strand exchange proceeds via several steps. First, a single-stranded DNA tail that is the result of processing by other factors is coated by ATP-bound RAD51 to yield a nucleoprotein filament. This filament then searches for a homologous sequence within duplex DNA, and catalyzes the exchange of strands between the single-stranded and double-stranded DNA (ssDNA and dsDNA) substrates. At the end of this process, the original broken end of the damaged DNA filament is aligned with an appropriate matching sequence in an intact duplex, and is further processed by other enzymes [55].
RAD51 possesses an ATPase domain that is structurally similar to the ATPase domains of helicases and of the F1 ATPase [56] and an N-terminal domain used for the interactions with DNA [57]. Electron microscopy studies have shown that RAD51 oligomerizes and forms helical filaments in which the DNA lies close to the filament axis [58]. As mentioned before, for the correct assembling of this filament onto the ssDNA it is required the presence of BRCA2.

2.4.3 Interaction between BRC4 and zone I and zone II of RAD51

As previously explained, BRCA2 binds the RAD51 monomers through 8 conserved motifs called BRC repeats. Out of these eight motifs, BRC4 is the one with the highest affinity for RAD51 and thus we focused our attention on its structure and its interactions with RAD51.
BRC4 binds RAD51 in two different hydrophobic pockets called zone I and zone II, respectively. Zone I pocket can lodge BRC4's FxxA motif (residues 1524−1527 of BRCA2) and binds directly to the oligomerization interface occupying two hydrophobic pockets. Those same pockets, in a RAD51 oligomer, are occupied by the RAD51's FTTA motif that mediates inter-subunit contact.
The zone II pocket can lodge the BRC4's LFDE motif (residues 1545−1548 of BRCA2), is situated far from the oligomerization interface and it is more evolutionarily conserved: mutations in this site causes cellular lethality and failure of RAD51 assembly in nuclear foci at the site of DNA breaks in vivo [59].
The BRC motif is characterized by hydrophobic residues that keep it in close contact with RAD51 throughout its length. Three main points of contact stand out, involving residues Phe 1524, Ala 1527, Leu 1545 and Phe 1546.
The first two mentioned residues interact with zone I: Phe 1524 is located on the strand of the β-hairpin contacting RAD51, and its aromatic ring is buried within a hydrophobic cavity formed by RAD51 residues. Ala 1527, in the second position of the hairpin loop, places its β-carbon into a small pocket formed by the side chains of other RAD51 residues.
The remaining residues are involved in the zone II interactions: Leu 1545 and Phe 1546 form a wedge embedded between RAD51 helices A4 and A5, and surrounded by residues Leu 204, Tyr 205, Ser 208 (in helix A4), and Met 251, Arg 254, Leu 255, Glu 258 and Phe259 (in helix A5) [60] [**Figure 2.7**].
For our project, in order to find an optimal RAD51-BRCA2 disrupting molecule, we focused on the synthesis of molecules that could bind these two zones and interfere with the protein-protein interaction.

During our researches, we managed to synthesize two types of compounds:
-Zone I inhibitors, who interfered with the interaction between BRCA2 and the zone I of RAD51.
-Zone II inhibitors, who disrupted the interaction between the Zone II of RAD51 and BRCA2.

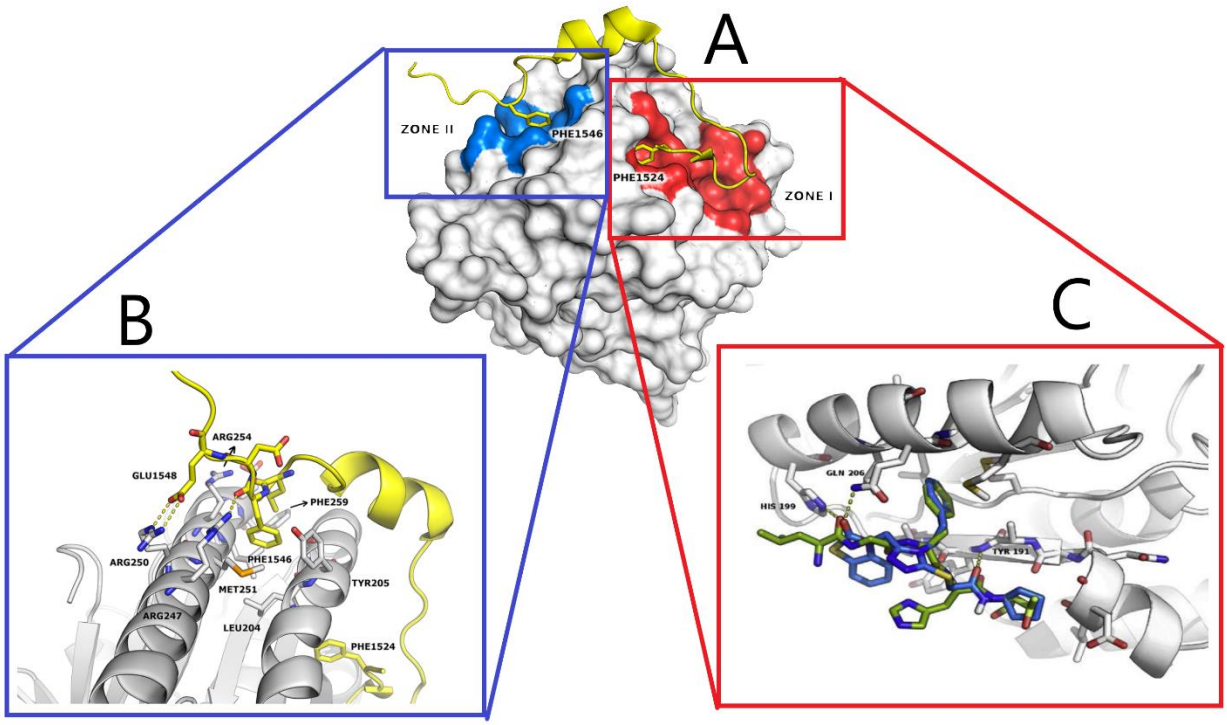

Figure 2.7. (*A***).** *Overview of the interactions between BRC4 (Yellow) and Zones I (Red) and II (Blue); RAD51 is represented as a white surface, BRC4 as a cartoon. (B). Zone II magnification showing the interacting residues of BRC4 (yellow) and RAD51 (white). (C). One of our compounds docked into the FxxA domain of RAD51. The small molecule recapitulates major interactions the peptide BRC4 establishes with the biological target.*

2.5 PROJECT B: INHIBITION OF HOMOLOGOUS RECOMBINATION ACTIVITY THROUGH THE USE OF LDH INHIBITORS.

2.5.1 Cancer: a metabolic disease

Many studies highlight that cancer can be considered a metabolic disease, characterized by aberrant and/or dysregulated glucose metabolism and bioenergetics. Neoplastic cells typically show highly increased rates of glucose uptake and glycolysis, after which the obtained pyruvate is converted to lactate by lactate dehydrogenase (LDH). [61]

In normal cells, under aerobic conditions, pyruvate is generated from glucose via glycolysis in the cytosol and is used to fuel oxidative phosphorylation, theoretically generating 36 net adenosine triphosphate (ATP) per molecule of glucose. Under anaerobic conditions, glycolysis is favored and relatively little pyruvate is dispatched to the oxygen-consuming mitochondria [62].

In cancer metabolism, one of the most well-known phenomena is the Warburg effect. In 1924, Otto Warburg observed that cancer cells consume much larger quantities of glucose than normal ones and metabolize it predominantly through glycolysis, thus producing high

levels of lactate even in oxygen-rich conditions, hence the term aerobic glycolysis [**Figure 2.8**] [63].

There are many reasons that explain why cancer cells tend to prefer aerobic glycolysis towards oxidative phosphorylation:

1- Aerobic glycolysis benefits cancer cells by avoiding generation of oxidative stress from the electron transport chain: this proves to be extremely useful in a condition when cells are constantly replicating [64].
2- The aerobic glycolysis provides the intermediates of the citric acid cycle for anabolic reactions to synthesize other organic molecules needed by the cell: glucose-6-phosphate can be oxidized and used to synthesize nucleotides for DNA and RNA. Dihydroxyacetone phosphate is the precursor for the biosynthesis of the fatty acids. 3-phosphoglycerate provides the carbons for cysteine, glycine and serine, whereas pyruvate provides the carbons for alanine [65].
3- The overexpression of glycolytic enzymes leads to accumulation of lactate, which causes acidification of the tumoral environment. Acidic extracellular pH is a major feature of tumor tissue and increases the expression of some genes (VEGF, IL-8) involved with pro-metastatic factors and can activate enzymes like metalloproteinase and cathepsins that disrupt the extracellular matrix [66].
4- Additionally, lactate itself functions as an intrinsic inflammatory mediator that increases interleukin (IL)-17A production by T-cells and macrophages; this results in the promotion of chronic inflammation in tumor microenvironments [67].
5- Cancer cells evade apoptosis under hypoxic conditions and acquired resistance to therapeutic agents. Among various mechanisms that contribute to the evasion of apoptosis in cancer, metabolism is emerging as one of the key factors. Cellular metabolites can regulate functions of pro- and anti-apoptotic proteins. In turn, p53, a regulator of apoptosis, also controls metabolism by limiting glycolysis and facilitating mitochondrial respiration. Consequently, with dysregulated metabolism and p53 inactivation, cancer cells are well equipped to disable the apoptotic machinery [68].

A malfunctioning in the oxidative phosphorylation does not cause the increase of the glycolytic pathway; in fact, the coexistence of increased glycolysis and oxidative phosphorylation is observed in some cancer cells, and these metabolic phenotypes can be induced to mutually switch in response to drug or micro-environmental stimulation [69]. This enhancement of glycolysis can be induced by hypoxia or hypoxia-induced factor 1 (HIF-1), even in the presence of fully functioning mitochondria, and is present in different heterogeneous cancer cells and in cancer-associated fibroblasts (CAFs) that also launch metabolic reprogramming to support cancer cell growth and metastatic dissemination. HIF-1 can increase the transcription of glucose transporters (GLUT1, GLUT3), many glycolytic enzymes and LDHA [70]. Normally HIF is induced in hypoxic situations but can be induced even under normoxic conditions by the glycolytic metabolites, pyruvate and lactate [71],

mTOR activation, NAD+ levels, many TCA cycle metabolites, oncogene gain of function and tumor suppressor gene loss of function [72].

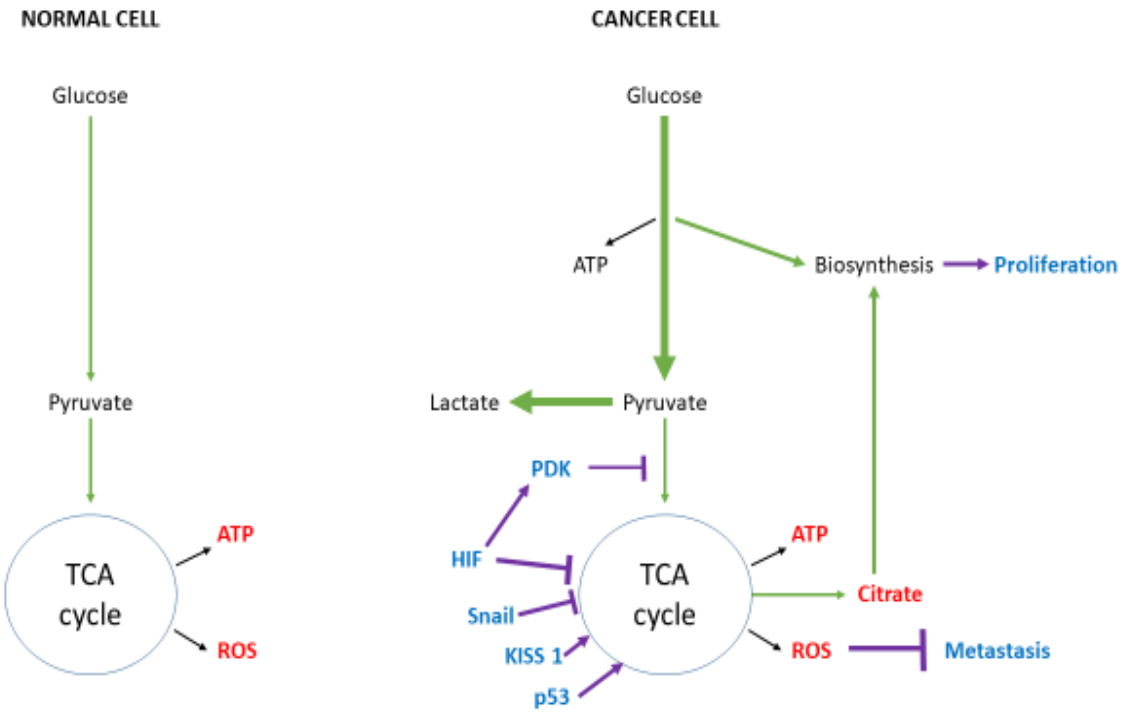

Figure 2.8. *Metabolic pathways of normal cells (to the left) and cancer cells (to the right).*

2.5.2 Lactate Dehydrogenase

Lactate Dehydrogenase (LDH) is an enzyme belonging to the oxidoreductase family. LDH inter-converts pyruvate and lactate using nicotinamide adenine dinucleotide (NAD^+), an essential cofactor that is required for a wide range of cellular reactions including ATP production.

LDH protein is a tetramer, its subunits are produced by three LDH-encoding genes (*LDH-a*, *LDH-b* and *LDH-c*) which produce the LDH-A, LDH-B and LDH-C subunits respectively. The three genetic loci show 71–75% sequence identity, indicating wide conservation in amino acid composition of the LDH subunits [73]. Isoform LDH-A is particularly interesting because it has been linked to an actively glycolytic metabolism since it favors the conversion from pyruvate to lactate under anaerobic conditions in normal cells [74].

The association of A and B isoforms can produce five isozymes: LDH-1 (A_0B_4), LDH-2 (A_1B_3), LDH-3 (A_2B_2), LDH-4 (A_3B_1) and LDH-5 (A_4B_0); The LDH forms enriched in A subunits are predominant in skeletal muscle and liver, while those enriched in B subunits are mainly found in heart and brain. Isozyme LDH-5 has been reported to be the primary form expressed in cancer cells [75]. The subunit LDH-C can only form a homotetramer and it is a testis specific isozyme. LDH-C is required for sperm to accomplish fertilization [76].

Regarding the structure of this enzyme, by looking at the crystal structures of the isoforms LDH-1 and LDH-5 we can identify two domains [77]:

1- NADH binding domain: this area is formed by residues 20–162 and 248–266 and is characterized by a 'Rossmann' fold, a region of the peptide where three parallel ß-strands enclose two alpha-helices. In this region, NADH binds in a groove of the central ß-sheet with the His195; Asp168, Arg171, Ile250 and Thr246 are essential residues to assemble the geometry of the catalytic site.
2- Substrate binding domain: it comprises the residues 163–247 and 267–331. The pyruvate binding cavity is located at the interface between the two domains, where residues 99–110 form the so-called 'active site loop'.

Recent experiments also evidenced for this enzyme a possible role beyond the mere management of pyruvate/lactate balance in glucose metabolism. In fact, similar to other glycolytic enzymes, LDH was found to be a protein "moonlighting" in cell nucleus, where it could bind to ssDNA and mRNA and take part in transcriptional complexes regulating gene expression [78]. The LDH-A subunit is an essential component of the transcriptional complex of the histone 2B gene (*H2B*): the subunit is associated with glyceraldehyde 3-phosphate dehydrogenase (GAPDH) and the coordinated activity of the two enzymes maintain the proper NAD+/NADH ratio necessary for optimal H2B protein expression [79]. LDHA with tyrosine phosphorylation has also been reported as localized to the nucleus, suggesting that tyrosine phosphorylation may play an essential role in LDHA function in the nucleus [80].

LDH appears to be one of the most interesting potential targets for designing an anti-metabolic cancer treatment. This enzyme is constantly overexpressed in cancer cells and, because of its position at the end of the glycolytic pathway, it is considered not necessary for the viability of normal cells, which mainly catabolize pyruvate via the TCA cycle [81]. Genetic studies also revealed that LDH-A knockdown inhibits in vitro and in vivo growth of certain cancer cell lines [82]. The most studied LDH inhibitor is Oxamate (OXA), a pyruvate analogue that inhibits LDH by substrate competition. Researchers demonstrated that downregulation of LDH-A by using both *LDH-a*-targeted siRNA and OXA increased tumoral cell death by apoptosis [83]. However, Oxamate is not suitable for in vivo therapies. In fact, it has limited cell penetration and therefore relatively high doses are required to have any significant effect. It is still highly use in in-vitro studies since it is highly specific and its mechanism of action is well known.

Recently, a promising LDH inhibitor potentially active in vivo has been synthetized: during the tests, the suppression of the glycolytic flux through inhibition of the conversion of pyruvate to lactate was observed in both in vitro and in vivo models, concomitant with disruption of the NAD^+/NADH ratio. In the used animal model, the only observed toxic

effect that could potentially narrow the therapeutic window of this novel compound was found to be hemolysis, presumably linked to the metabolic inhibition of red blood cells [84].

2.5.3 Correlations between LDH activity and DNA repair mechanisms

As previously mentioned, the enhanced glycolysis activity promotes various cancer-essential functions other than just providing the cells with higher levels of ATP. One of these functions in particular is highly relevant for the purpose of this project: the maintenance of tumoral DNA integrity. This is a crucial function for supporting active proliferation, even for cancer cells already bearing genetic mutations. Studies mention that when glycolysis activity is increased, cancer cells become more proficient in repairing DNA damage and more resistant to ionizing radiation [85]. Likewise, considerable amounts of evidences suggest that inhibition of glycolysis leads to compromised DNA repair [86].

Despite all this evidence, the mechanisms linking the glycolysis-based metabolic program to DNA repair mechanisms have not been fully understood. A possible explanation could reside in the depletion of ATP, since without energy cells would not be able to repair its genome. Moreover, an involvement by LDH's moonlight activities (mentioned in the previous chapter) or by its product, the lactate, must be considered.

Lactate is highly produced in tumoral environment and is one of the factors that promote cell invasion via acidification of the extracellular matrix. Moreover, lactate can also affect gene transcription by influencing the activity of histone proteins.

Histone modification by acetylation is an important process in transcriptional regulation. The chromatin of transcriptionally active genes is epsilon-amino (ε-NH 2) acetylated on the N-terminal tails of histone H3 and histone H4, whereas that of inactive genes is hypoacetylated. Histone modification and gene regulation arise from the differential recruitment of histone acetyltransferase (HAT) and histone deacetylase (HDAC) enzymes to chromatin. Lactate can inhibit the activity of HDAC proteins and indirectly regulate gene expression; it is important to note that expression changes induced by lactate correlate with changes induced by other HDAC inhibitors across the entire genome [87].

Furthermore, lactate can induce even lactylation of histone's lysine residues: this lactylation process serves as an epigenetic modification that directly stimulates gene transcription from chromatin and is remarkably dependent by cellular glycolysis activity [88].

Even though the molecular mechanisms that link the glycolytic pathway and the DDR pathways are not fully clarified, it is possible that inhibition of LDH could be a valuable method to obtain HR inhibition and enhance the effect of PARP inhibitors.

3. SPECIFIC AIMS

In the past two decades, research has focused on discovering tumor-specific signaling and metabolic pathways that might be exploited for pathway-targeted anticancer therapies. Currently, several small molecules and monoclonal antibodies have been approved, which directly inhibit genes and proteins that are critical in oncogenic signal networks. These have increased survival in patients with previously intractable cancers. However, the first generation of targeted therapies have some limitations, including the development of resistance and on- and off-target toxicities. For these reasons, researchers are increasingly turning to precision medicine, using genetic changes in a patient's tumor to determine their treatment. Synthetic lethality is a new concept with great potential for discovering new anticancer molecules within the framework of precision medicine.

Synthetic lethality arises when a combination of mutations in two or more separate genes leads to cell death, while the single mutated genes do not affect the viability of the cell.

Using this concept, new anti-cancer strategies that target specific gene defects can be implemented, such as the use of OLA in BRCA-less cancer cells. The advantage of those therapies is that only cancer cells suffer an increase in cell death while normal cells are spared. Unfortunately, their use is limited only in tumors whose cells carry the desired mutation.

In this thesis, we present a new working hypothesis dubbed “fully small-molecule induced synthetic lethality”. With this hypothesis, we want to prove that it is possible to strengthen the effect of OLA in BRCA-proficient tumors using compounds that can interfere with the HR mechanism.

In order to achieve HR inhibition, we used two different approaches.

In the direct approach (**Project A**), we used RAD51-BRCA2 disruptors. This protein-protein interaction is a focal point in the repair of DNA double strand damage; therefore, disruptors should be able to mimic a BRCA-less cellular environment. We focused our research on compounds that could bind to Zone I and II of RAD51, the two hydrophobic pockets that interact with BRCA2.

The efficacy of new synthetized RAD51-BRCA2 disruptors was tested by comparing their effects on cell lines with different DNA repair efficiency:

- BxPC3: a BRCA2 competent cell line
- Capan-1: a cell line expressing a non-functional BRCA2 protein

In the indirect approach (**Project B**), we inhibited HR by interfering with the cellular metabolism through inhibition of LDH activity. Various studies suggest a possible connection between the activity of this enzyme and the efficiency of DNA repair pathways.

In order to evaluate the effect of LDH inhibition on HR, we decided to use cells characterized by different metabolic asset:

- BxPC3: a cell line that relies mostly on LDH activity and glycolysis for its energy metabolism
- SW620: a cell line showing an energy metabolism more dependent on oxidative reactions

Both **Project A** and **project B** have the same objectives:
1. To characterize the in vitro effects of the tested compounds on the HR mechanism
2. To determine if their activity on the HR mechanism could effectively mimic a BRCA-less environment and induce synthetic lethality by administering them alongside OLA.

It is important to note that, in the original PARPi therapies, only cells bearing BRCA mutations were affected by OLA, while our new approach would target both normal and cancer cells. However, cancer cells rely on DDR pathway and LDH activity more often than normal cells. Therefore, our compounds should have an impact mostly on cancer cell survivability.

4. MATERIALS AND METHODS

4.1 Cell Culture

For the experiments we used two different pancreatic adenocarcinoma cell lines, BxPC3 and Capan-1, a human colon adenocarcinoma cell line called SW620 and a normal immortalized cell line called HK-2. The cell lines were obtained from ATCC.
BxPC3 cell line was derived from a 61-year-old woman and expresses a functional BRCA2 protein. Capan-1 cell line harbors a single base-pair deletion in the BRCA2 allele, which results in the expression of a truncated and dysfunctional protein.
Both pancreatic cell lines were grown in RPMI 1640 containing 10% FBS, 100 U/ml penicillin/streptomycin and 2 mM glutamine. The media and the other supplements were obtained from Sigma-Aldrich.
Non-neoplastic, immortalized cells from human kidney, HK-2, were grown in DMEM/F-12 containing 40 ng/mL dexamethasone, while SW620 cells were grown simply in DMEM; both of these media have been supplemented with 10% FBS, 100 U/ml penicillin/streptomycin and 2 mM glutamine.
In the experiments that involved OLA, media were supplemented with 0.6% DMSO; the same amount of DMSO was added to the untreated cultures as well.

4.2 Viability Assays

4.2.1 CellTiter-Glo ATP Assay

CellTiter-Glo Luminescent Cell is a Viability Assay developed by Promega. For this experiment, 1 x 10^4 cells in 200 μl of culture medium were seeded into each well of a 96-multiwell white body plate and allowed to adhere overnight. The following day the cells were treated with the desired compounds, administered alone or in combination. After the incubation, whose time differed based on the various experiments, the plate was allowed to equilibrate for 30 min at room temperature and then 100 μl CellTiter-Glo reactive were directly added to each well. The plate was kept on a shaker for 2 min followed by 10 min of incubation at room temperature, to induce cell lysis. Luminescence was measured by using a Fluoroskan Ascent FL reader (Labsystems).

4.2.2 Neutral Red Assay

Cells (1-2 x 10^4/well) were seeded in two 96-well plates. At the end of the treatment, cells were maintained in medium containing 30 μg/ml Neutral Red for 3 h. Medium was then removed and the cells were solubilized with 200 μl of 1% acetic acid in 50% ethanol. The absorbance of the solutions was measured at λ=540nm using a microplate reader (Multiskan

EX, ThermoLab Systems). To estimate cell numbers, before each experiment a plot reporting the Neutral Red absorbance values obtained from scalar amounts of cells was acquired.

4.3 Lethality assays

4.3.1 CellTox™ Green Cytotoxicity Assay

Cells (1 x 10^4/well) were plated in 96-well plates and treated with the desired compounds, given alone or in combination. At the end of treatment, the CellTox™ dye was added to cell cultures and the green fluorescence signal, which is produced by the binding interaction with dead cell DNA, was measured using an EnSpire 2300 multilabel reader (Perkin Elmer) with a 512nm excitation wavelength and a 532nm emission wavelength. As a positive control, cells were treated with lysis buffer 1:50 (Promega).

4.3.2 Vital dyes assay

Cells were grown on coverslips placed in a 6-multiwell plate (5 x 10^5 cells/well). After a 48h/72h treatment with the desired compounds, given alone or in combination, wells were rapidly washed with PBS and filled with 500 µl of PBS solution containing 4′,6-diamidino-2-phenylindole (DAPI, 4.6 µg/ml) and propidium iodide (PI, 50 µg/ml). After a 10 min incubation at room temperature under light-shielded condition, BxPC3 cells were washed with PBS, fixed (10 min) with 10% neutral buffered formalin solution and washed again to eliminate excess fixative. Coverslips were then applied on glass slides using two drops of mounting media: 200 µg/ml 1,4-diazabicyclo[2.2.2]octane (DABCO) 20 mM Tris-HCl, 90% glycerol. Images were acquired on a Nikon fluorescent microscope equipped with filters for DAPI and PI.

4.4 Homologous recombination Assay

Homologous recombination (HR) efficiency was assessed by using a commercially available assay (Norgen). This assay is based on cell transfection with two plasmids that, upon cell entry, can recombinate. The HR product can be assessed by both PCR and real time PCR, using primer mixtures included in the assay kit. Different primer mixtures allow to discriminate between the original plasmid backbones and their recombination product.
BxPC3 and SW620 cells (2 × 10^5 per well) were seeded in a 24-well plate and allowed to adhere overnight. Co-transfection with the two plasmids was performed in Lipofectamine 2000 (Invitrogen), according to the manufacturer's instructions and left for 5h. Cells were exposed to different doses of treatments, dissolved in RPMI in the presence of 0.6% DMSO and the incubation time lasted either 5h or 16h. After washing with PBS cells were harvested

and DNA was isolated using Illustra^{TM} Tissue and Cell Genomic Prep Mini Spin kit (GE Healthcare). Sample concentration was measured using an ONDA Nano Genius photometer.
In the first experiments, the efficiency of HR was assessed by standard PCR performed according to the manufacturer's instructions and using 100-150 ng of template. The amplicons of plasmid backbones and of recombination product were separated by electrophoresis on 2% agarose gel. Band intensity was measured by Kodak Electrophoresis Documentation and Analysis System (EDAS) 290 and used to evaluate HR efficiency, which is given by the ratio: [Recombination Product/Backbone Plasmids].
In further experiments, to improve data quantification, the same assay was performed using real-time PCR.
Real-time PCR was performed by using 25 ng of template, the primer mixtures included in the assay kit and following the protocol indicated by the manufacturer. Data analysis was based on the ΔΔCt method: [Recombination Product / Backbone Plasmids] ^{treated} versus [Recombination Product / Backbone Plasmids] ^{control}.

4.5 Western Blot analysis

Cell cultures (1.5 x 10^6 cells) were exposed to the desired compounds, given alone or in combination. After the incubation, cells were lysed in 60-100 µL RIPA buffer containing protease and phosphatase inhibitors (Sigma Aldrich). The homogenates were left 30 min on ice and then centrifuged 15 min at 10000 g. From 30 µg to 50 µg proteins of the supernatants (measured according to Bradford) were loaded into 4-12% polyacrylamide gel for electrophoresis and run at 170V. The separated proteins were blotted on a low fluorescent PVDF membrane (GE Life Science) using a standard apparatus for wet transfer with an electrical field of 80 mA for 16 h. The blotted membrane was blocked with either 5% BSA in TBS-Tween, or 2.5% BSA and 2.5% Casein in TBS-Tween depending on the antibody, and probed with the primary antibody. The antibodies used were: rabbit anti-γH2AX [phosphor S139] (Abcam), mouse anti BCL-2 (Santa Cruz), rabbit anti BAX (Abcam), rabbit anti-Actin (Sigma Aldrich). Binding was revealed by a Cy5-labelled secondary antibody (anti rabbit-IgG, GE Life Science; anti mouse-IgG, Jackson Immuno-Research). All incubation steps were performed according to the manufacturer's instructions. Fluorescence of the blots was assayed with the Pharos FX scanner (BioRad) at a resolution of 100 µm, using the Quantity One software (BioRad).

4.6 Micronuclei visualization

For micronuclei visualization, BxPC3 cells were grown on coverslips placed in a 6-multiwell plate (5 x 10^5 cells/well). After a 72 h treatment with olaparib and/or RAD51-BRCA2 disruptors, cells were rapidly washed with PBS and then fixed for 10 min with cold methanol. Coverslips were then air-dried and mounted on glass slides using DAPI (5 µg/ml)

DABCO solution (described in 3.3.2 paragraph). Images were acquired on a Nikon fluorescent microscope equipped with filters for DAPI.
A cell was considered to contain micronuclei if the following criteria were met: (i) one or more round fluorescent bodies were present in the cytoplasm, which did not touch the main nucleus; (ii) they were < 1/3 of the main nucleus diameter; and (iii) they were nonrefractile, to exclude foreign bodies. Two independent observers estimated the percentage of cells bearing micronuclei, by analyzing 100-250 cells for each treatment sample.

4.7 Immunofluorescence experiments

Immunofluorescence was used for studying RAD51 nuclear translocation and for evaluating DNA damage through the detection of γH2AX nuclear foci.
To visualize RAD51 in cell nuclei, the cells were seeded on glass coverslips placed in a 6-well culture plate (2×10^5 cells/well) and allowed to adhere overnight. Cultures were then preincubated with ARN 24089 (1h incubation) or OXA (16h incubation) and subsequently exposed to 50 μM cisplatin for an additional 1.5 h. Medium was removed, and cells were maintained in the presence of ARN 24089 or OXA for 4h/5h. After this time, cultures growing on coverslips were fixed in PBS containing 1% formalin for 20 min, permeabilized in 70% ethanol, air-dried, and washed twice with PBS. Samples were incubated in 10% bovine serum albumin (BSA) in PBS for 30 min at 37 °C and subsequently exposed to an anti-RAD51 mouse monoclonal antibody (Santa Cruz Biotechnology, 1:1000 in 5% BSA/PBS) overnight at 4 °C. After washing, coverslips were incubated with an anti-mouse FITC-conjugated secondary antibody (1:1000 in 1% BSA/PBS) for 1 h at 37 °C, washed, air-dried, and mounted with a solution of DAPI (2 μg/mL) and DABCO solution (described in 3.3.2 paragraph).
To evaluate DNA damage through γH2AX nuclear foci, BXPC3 and Capan1 cells were seeded on glass coverslips in 6-well tissue culture plate (2×10^5 cells/well) and allowed to adhere overnight. After 48 h treatment with OLA (10 μM) or ARN 24089 (20 μM) given alone or in combination, cultures growing on coverslips were fixed and treated as described above. For this experiment, the used antibodies were a rabbit polyclonal anti-γH2AX (Abcam, 1:1000 in
5% BSA/PBS) and a secondary anti-rabbit rhodamine-labeled (Novus Biologicals, 1:1000 in 1% BSA/PBS). For both experiments, images were acquired using a Nikon fluorescent microscope equipped with filters for FITC, TRITC, and DAPI. The percentage of cells bearing
nuclear foci was estimated by two independent observers, by analyzing 100−250 cells for each treatment sample.

4.8 Real-Time PCR

Cells were seeded in T25 flasks (7 x 10^5 cells / flask) and allowed to adhere overnight. Cultures were then exposed to oxamate for additional 16 h: a 40 mM dose was used for SW620 cells; 20 mM for BxPC-3 cells. RNA was extracted using the PureZOL isolation reagent (Bio-Rad) and was quantified spectrophotometrically. Retro-transcription to cDNA was performed by using the Revert Aid™ First Strand cDNA Synthesis Kit (Thermo Fisher Scientific), in different steps: 5 min denaturation at 65°C, 5 min annealing at 25°C, 1 h retro-transcription at 42°C and 5 min inactivation at 70°C. Real Time PCR analysis of cDNA (15 ng) was performed using SYBR Green Supermix (SSO Advanced, BioRad). The sequence of primers used for analyzing expression of the studied proteins and of the internal control genes are reported in **Table 4.1**.
For all examined genes, annealing temperature of primers was 60°C and the thermal cycler (CFX96 ™ Real Time System, BioRad) was programmed as follows: 30 sec at 95°C; 40 cycles of 15 sec at 95°C; 30 sec at 60°C.

Table 4.1. *List of primer sequences used for RT-PCR analysis.*

Gene	Forward primer (5' – 3')	Reverse primer (5' – 3')
LDH-A	GACCTACGTGGCTTGGAAGA	TCCATACAGGCACACTGGAA
LDH-B	CCAACCCAGTGGACATTCTT	AAACACCTGCCACATTCACA
BRCA1	TATCCGCTGCTTTGTCCTCA	TGCAGGAAACCAGTCTCAGT
BRCA2	GAGAGTTCCCAGGCCAGTAC	ACTGGAAAGGTTAAGCGTCA
NBN (Nibrin or P95)	CCACCTCCAAAGACAACTGC	TCAGGACGGCAGGAAAGAAA
MRE11 (Double Strand Break Repair Nuclease)	TGTTGAGGTTGCCATCTTGA	TGATCAGTCAGTCAACTTTGGT
RAD50 (Double Strand Break Repair Protein)	CTGCTTGTTGAACAGGGTCG	CCAATTCTAGCTGTGTTGCCA
RAD51 (Recombinase)	CAAATGCAGATACTTCAGTGGAA	TCCAGCTTCTTCCAATTTCTTCA
DCLRE1C (DNA cross-link repair 1C or Artemis)	TTCTCCCTATCGAAGCGGTC	ATGAGTTCTTTCGAGGGGCA
LIG4 (DNA Ligase 4)	GGTCGTTTACTTGCTGTATGGT	TGCATATTTTGTGTTGAAGCCA
PRKDC (DNA-PK)	GAGCTCAACGTACATGAAGTCA	TGTGGATTCGAACAACAAGGAG
XRCC4 (X-ray repair cross complementing 4)	GCATTGTTGTCAGGAGCAGG	TGAAGGAACCAAGTCTGAATGAG
XRCC5 (X-ray repair cross complementing 5 or Ku80)	AGAATCCCCATTTGAACAAGCA	GAAAGGGGATTGTCAGTGCC
XRCC6 (X-ray repair cross complementing 6 or Ku70)	GGGCAAGATGAAGGCTATCG	GTTCCGGCTCCATCAAATCC
LIG1(DNA Ligase 1)	CACCACTCCATTCCACTCCT	AGGGAGAATTCTGACGCCAA
PARP1 (Poly(ADP-ribose) polymerase 1)	GCTATCATCAGACCCTCCCC	GGTGGAAATGCTTGACAACCT

WRN (Werner syndrome RecQ like helicase)	AGTTCTTGTCACGTCCTCTGG	GGTGCCTATTTAAGTTAATGTCTGC
XRCC1 (X-ray repair cross complementing 1)	TCCCAATGTCCACACTGTGT	TCAAGGCAGACACTTACCGA
CYP33A (Cyclophilin 33A)	GCTGCCTGTGCACTCATGAA	CAGTGCCATTGTGGTTTGTGA
GUSB (Glucuronidase Beta)	CTCATTTGGAATTTTGCCGATT	CCGAGTGAAGATCCCCTTTTTA
RPS13 (Ribosomal Protein S13)	CCCCACTTGGTTGAAGTTGA	ACACCATGTGAATCTCTCAGGA
TUBA (Tubulin Alpha)	TGGAACCCACAGTCATTGATGA	TGATCTCCTTGCCAATGGTGTA

4.9 Measurement of lactate levels

For this assay, 5 x 10^5 cells were seeded in 6-well plates and opportunely treated the day after in triplicate. At the end of the treatment, the medium was replaced with 1 ml of Krebs-Ringer buffer (118 mM NaCl, 4.7 mM KCl, 3.4 mM $CaCl_2$, 1.2 mM KH_2PO_4, 1,2 mM $MgSO_4 \bullet 7H_2O$, 24.6 mM $NaHCO_3$, glucose 4 mg/ml) and scalar concentrations of OXA. Lactate levels were measured in two untreated wells at the start of experiment (baseline value) and 3h (or 6h) after incubation at 37°C.

At the end of incubation 100 μl of 100% trichloroacetic acid (TCA) was added to each well. Therefore, the cells were collected, lysated and centrifuged at 1700g for 5 minutes. At the end of the centrifugation, the lactate in the supernatant was measured according to the method of Barker and Summerson [91]. The amount of metabolite formed during the 3h incubation with or without the LDH inhibitor was calculated from a standard curve and subtracting the baseline value. The lactate concentration in the various samples and in the standard curve was read with a spectrophotometer at λ=565nm.

4.10 Statistical analysis

All data were analyzed by using the Prism 5 GraphPad software. Each experiment was performed with triplicate samples per treatment group. Results are expressed as mean ± SE of replicate values; p values < 0.05 were considered statistically significant.

4.11 Combination Index

The interaction index between OLA and RAD51-BRCA2 disruptors/OXA was assessed by applying the following formula:

(Surviving cells treated with combination) / [(Surviving cells treated with OLA) X (Surviving cells treated with Rad51-BRCA2 disruptor/OXA)]

As described in the paper [89], a result ranging from 0.8 to 1.2 denotes an additive effect. Synergism is indicated by a result <0.8; antagonism by a result >1.2.

5. RESULTS AND DISCUSSION

5.1 PROJECT A: INHIBITION OF HR THROUGH THE USE OF RAD51-BRCA2 DISRUPTORS

5.1.1 ZONE I RAD51-BRCA2 DISRUPTORS

Targeting protein-protein interactions (PPI) is an attractive strategy for designing innovative drugs. However, it is rather difficult to identify and optimize PPI disruptors. This is because proteins usually interact with other proteins via shallow surface sites. In a previous work, researchers from Italian Institute of Technology and from FaBiT department of the University of Bologna identified a potentially suitable pocket, often referred to as the "FxxA pocket"(zone I). This zone is one of the two RAD51 regions where BRC4 (i.e. the fourth BRC repeat responsible for binding of BRCA2 to RAD51) binds its counterpart. After a virtual screening campaign based on high-throughput docking at the FxxA pocket a series of triazole-based compounds were identified. Subsequent ELISA biochemical assay and biological assay showed that two of them were able to disrupt the RAD51-BRCA2 interaction and therefore were selected as initial hit compounds.
Notably, triazoles bear a peculiar structure that makes them particularly suited to disrupting protein-protein interactions. In fact, the binding mode to RAD51, as obtained by docking simulations, shows noticeable similarities to the crystallographic structure of RAD51 in complex with BRC4. To improve the protein-protein inhibitory activity of those two molecules, a chemical modification campaign was conducted around the triazole moiety and new analogues were synthesized. To investigate their mechanism of action, the ability of compounds to inhibit RAD51-BRCA2 interaction was investigated with a competitive biochemical ELISA assay in comparison initial hit compounds. This assay is effective in evaluating the ability of new molecules to compete with BRC4 to bind to RAD51.

5.1.1.1 Preliminary selection of Zone I disruptors

The most promising compounds at the ELISA assay (ARN 21560, ARN 21627, ARN 21689 and ARN 21730) were submitted to cell-based studies. ARN 21689 and ARN 21730 were discarded because of poor solubility. The remaining two compounds were characterized in human pancreatic carcinoma, using BxPC3 cells [**Table 5.1**]. These cells were chosen for their clinical relevance and for the possibility of using Capan-1 cells, which lack functional BRCA2 protein and could therefore serve as negative control. Additionally, BxPC3 and Capan-1 match well in terms of tumor type and differentiation state.

Table 5.1. . *List of tested compounds and respective IC_{50}*

Compounds	IC_{50} Elisa	IC_{50} Viability
ARN 21560	10 µM	37 µM
ARN 21627	29 µM	>50 µM
ARN 21689	42 µM	N.S.[a]
ARN 21730	33 µM	N.S.[a]

[a]*N.S.=Not Soluble in the cell medium.*

The RAD51-BRCA2 interaction is crucial in recruiting the recombinase RAD51 to cell nuclei, where it uses homologous recombination (HR) to repair double-strand breaks. We therefore studied HR inhibition in BxPC3 and Capan-1 cells. The assay is based on cell transfection with two plasmids bearing the LacZ sequence, each with a different mutation. In transfected cells, the recombination machinery restores the corrected LacZ sequence, which can be detected by PCR. Using two different primer sets, both the plasmid couple and the recombination product can be measured, allowing an estimation of HR efficiency.
Both compounds reduced HR in treated BxPC3 cells suggesting their potential ability to disrupt RAD51-BRCA2 interaction in living cells too. Of the two molecules, ARN 21560 had the strongest effect, with a statistically significant 40% inhibition at 20 mM. ARN 21627 showed a less marked effect, with a 24% inhibition at 40 mM. The limited solubility of ARN 21627 further hindered a dose escalation with this compound. [**Figure 5.1**].

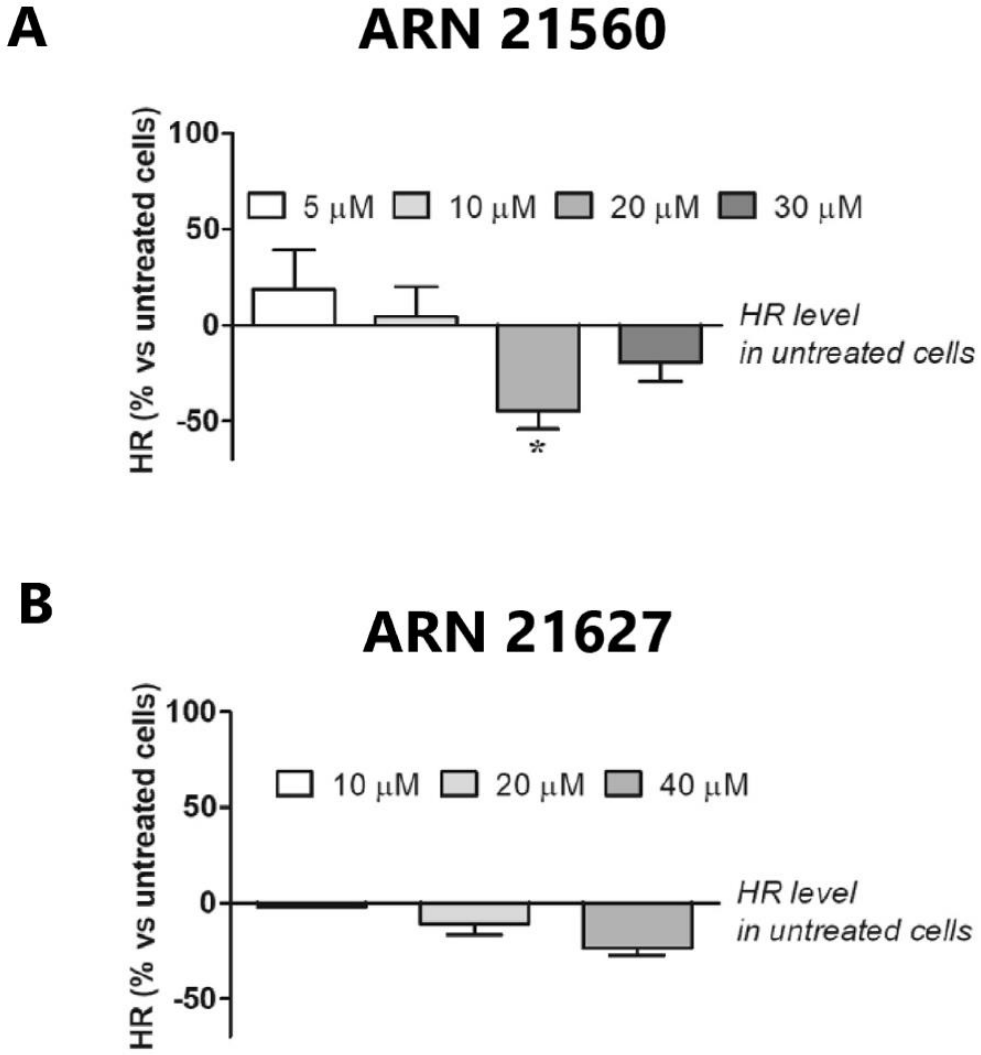

Figure 5.1. *Estimation of homologous recombination efficiency in BxPC-3 cells treated (16 h) with the newly identified BRCA2-RAD51 disruptors ARN 21560 (A) and ARN 21627 (B). *, p < 0.05 as evaluated by ANOVA followed by Dunnet's post-test.*

The HR data suggested that ARN 21560 and ARN 21627 were potentially capable of synergizing with OLA in pancreatic cancer cells with functional BRCA2, where OLA usually is inactive. The two compounds were therefore tested in BxPC3 and Capan-1 cell viability experiments in combination with OLA.

After 72 h of treatment, ARN 21627 did not affect the efficacy of OLA [**Figure 5.2, B**]. Conversely, ARN 21560 significantly increased OLA's efficacy in BxPC3 cells, without affecting its efficacy in the BRCA2-defective cells (Capan-1) [**Figure 5.2, A**].

These results further confirmed, in a dose-dependent manner, that HR inhibition might explain the synergistic effect of combining RAD51-BRCA2 disruptors with PARP inhibitors in cell lines with fully functional BRCA2, where PARP inhibitors are usually inactive. Further experiments were conducted on ARN 21560 to confirm the synergy with OLA.

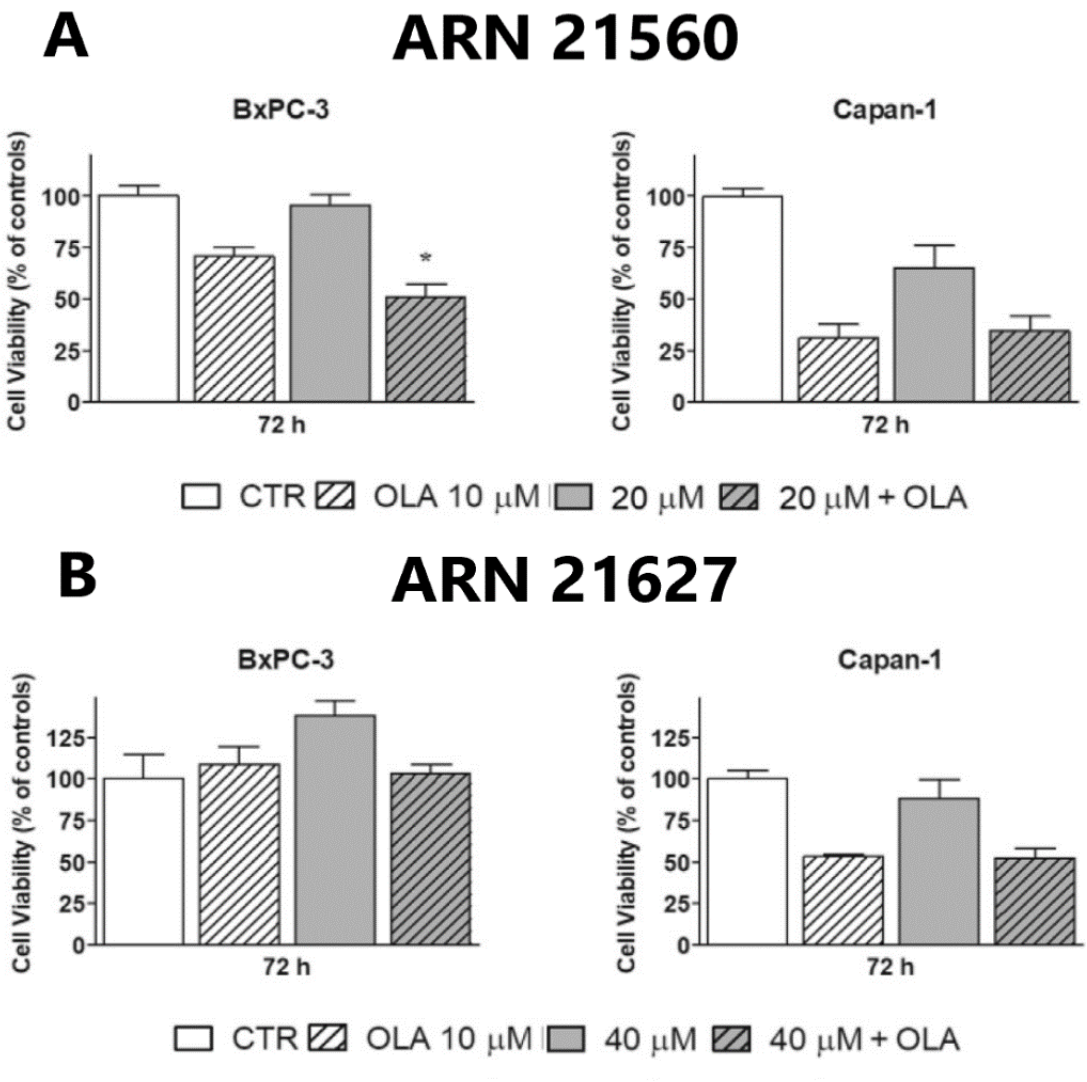

Figure 5.2. *Evaluation of cell viability assessed in combination experiments with OLA (10 mM) + ARN 21560 (A) or ARN 21627 (B) on BxPC-3 and Capan-1 cultures. The doses showing the best results in the experiments were used. *, p < 0.05 as evaluated by ANOVA followed by Dunnet's post-test.*

5.1.1.2 Western Blot analysis on γ-H2AX bands

Using the same exposure time we used in the previous experiments, an immunoblotting evaluation of DNA damage was also performed by measuring the phosphorylation of H2AX (γ-H2AX), a sensitive and universal indicator of DNA double-strand break formation.
The densitometric evaluation of γ-H2AX bands, normalized on actin levels, have been plotted in the bar graph. It shows that, in cells treated with the combination of OLA with ARN 21560, the DNA damage signal was >70% higher than the one observed in control and in OLA-treated cells. This experiment also showed that, when given as a single treatment, ARN 21560 did not cause appreciable signs of DNA damage. [**Figure 5.3**].

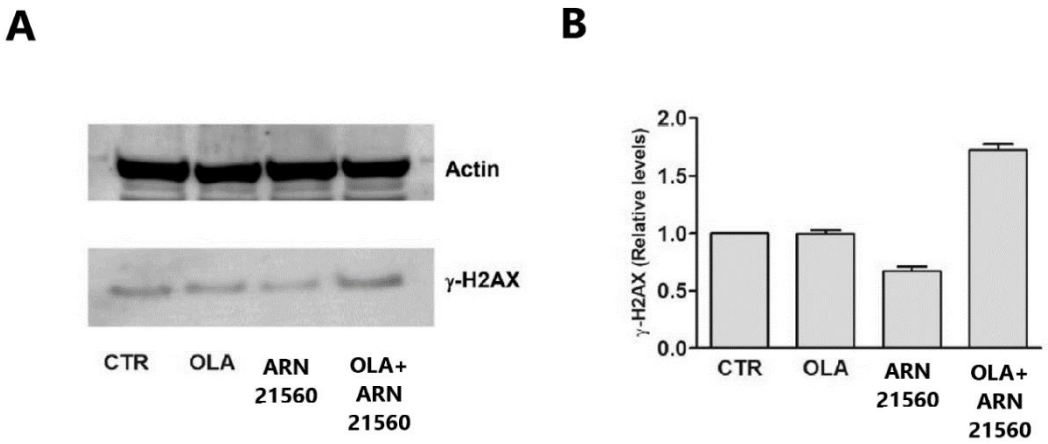

Figure 5.3. (*A*). *Western blot showing Actin bands and γ-H2AX bands: samples were isolated from BxPC3 cells treated for 144h with 10 μM OLA and 20 μM ARN 21560. (B). graph showing the intensity of the γ-H2AX bands, normalized on Actin levels.*

5.1.1.3 Lethality Assay on BxPC-3 and Capan-1 cells

Further experiments were conducted on ARN 21560 to confirm the synergy with OLA.
By adopting a longer exposure time to treatments (144 h), we assessed how the ARN 21560+OLA combination affected cell viability and cell death. Cell death was evaluated using the CellTox Green Dye (Promega) probe, which emits a fluorescence signal only in the presence of cells with impaired membrane integrity. Again, we observed a statistically significant increase in OLA's power in reducing cell viability. The data of the cell viability experiment were also used to evaluate the combination index (CI) between OLA and ARN 21560. According to this method, CI < 0.8 indicates synergism while a result ranging from 0.8 to 1.2 indicates additive effects. A CI value of 0.76 ± 0.03 was obtained, which suggests yet again a potential synergistic effect between the compounds.
However, when we analyzed the data obtained from the lethality assay, the enhanced OLA potency did not produce evidence of increased cell death. Despite the results obtained in the previous experiments, we could not fully reproduce the paradigm of synthetic lethality with ARN 21560. [**Figure 5.4**].

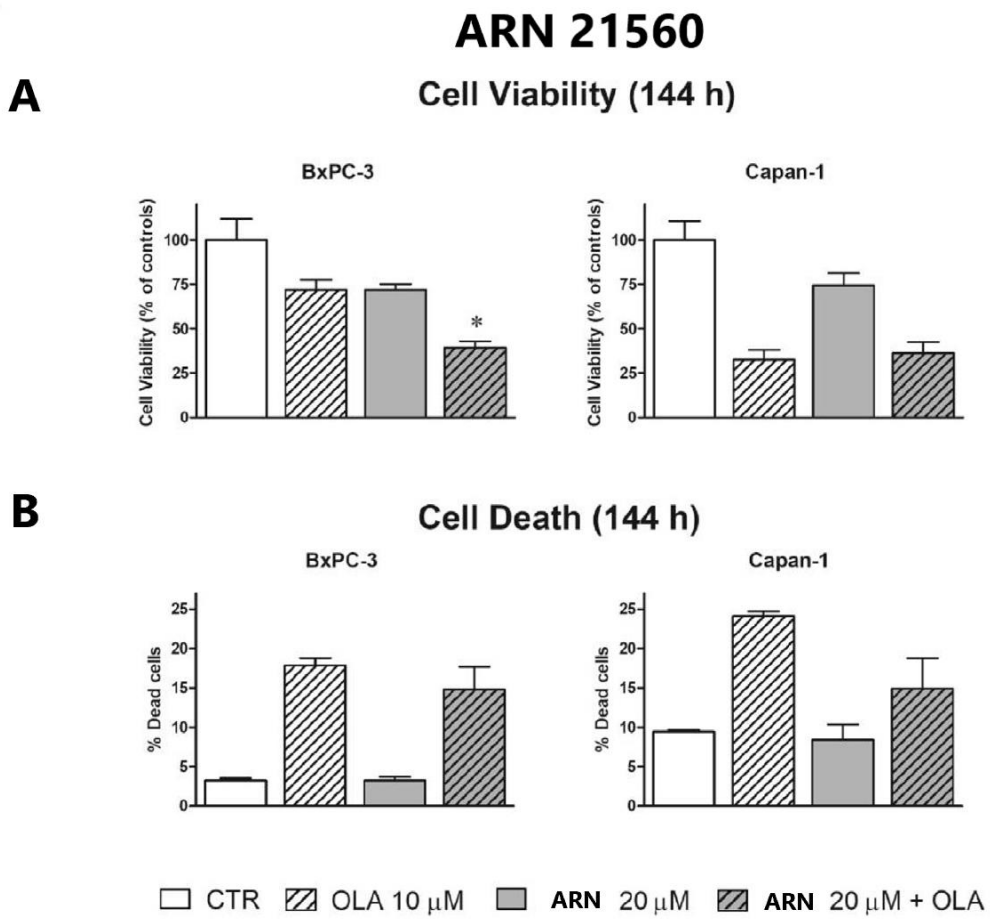

Figure 5.4. (*A*). *Viability data showed for comparison: BxPC3 and Capan-1 cells treated for 144h with 20 µM ARN 21560 and 10 µM olaparib (*: p < 0.05 evaluated by ANOVA followed by Dunnet's post-test).* (*B*). *Cell death data: BxPC3 and Capan-1 cells treated for 144h with 20 µM ARN 21560 and 10 µM olaparib.*

5.1.1.4 Project A final discussion (Zone I disruptors)

In recent years, innovative anticancer treatments have relied on targeted therapies to improve drug efficacy and reduce side effects. In parallel, precision medicine has provided a new paradigm for identifying individual patients or groups of patients for treatment with tailored pharmacological medications. For example, PARP inhibitors were recently been approved to treat ovarian cancer in patients with genetic mutations in the BRCA genes (1 and 2).
This has been demonstrated in ovarian cancer (for which OLA was originally approved), and in clinical trials in breast and pancreatic cancers. Pancreatic cancer is a major unmet medical need. Our work is based on a new paradigm dubbed "fully small-molecule induced synthetic lethality." This paradigm was based on the assumption that, by using a small organic molecule to disrupt the RAD51-BRCA2 interaction, it is possible to mimic the effect of BRCA2 germline mutations, thus widening the population of patients eligible for treatment with OLA and other PARPi.
In the first part of this study, we improved the biological screening cascade with experiments designed to confirm the molecular mechanism of action (disruption of RAD51-BRCA2 interaction) in cancer cells. We obtained one molecule, ARN 21560, with an improved profile

relative to the initial hits (according to a biochemical ELISA essay) and a clear mechanism of action, allowing synergy with OLA in pancreatic cancer cells (BxPC3) where OLA is normally inactive.

Given our initial results, we could conclude that ARN 21560:

1- inhibited the RAD51-BRCA2 interaction,
2- hit its target and inhibited its function in living cells,
3- significantly increased the therapeutic power of OLA alone in cells with a functional RAD51-BRCA2 pathway, where usually OLA is inactive,
4- increased the formation of double-strand breaks when administered in combination with OLA.

Unfortunately, the lethality experiments showed that OLA-ARN 21560 association did not trigger synthetic lethality. This could have been due to the low-level potency of our disruptor, which did not cause HR inhibition greater than 40%. In addition, the inherent resistance to apoptosis of BxPC3 cells, which bear a mutant p53, could have further prevented the synthetic lethality mechanism.

5.1.2 ZONE II RAD51-BRCA2 DISRUPTORS

In a second step of our work, with the intention of identifying novel RAD51-BRCA2 disruptors, researchers from Italian Institute of Technology and FaBit department of University of Bologna used the available X-ray crystallographic structure of the fourth BRC repeat (BRC4) in complex with the catalytic domain of RAD51. They performed a second virtual screening campaign targeting the LFDE binding pocket (Zone II). This binding pocket is more evolutionarily conserved than the FxxA (Zone I). Furthermore, mutation at the LFDE causes cellular lethality and failure of RAD51 assembly in nuclear foci at the site of DNA breaks in vivo. This further suggests this pocket has a critical site for RAD51's mechanism of action. To the best of our knowledge, no inhibitor that binds the LFDE binding pocket has been reported so far in the literature.
IIT researchers selected, purchased, and tested 42 small molecules for their inhibitory activity using a competitive biochemical ELISA assay. Among the tested compounds, a commercially available dihydroquinolone pyrazoline derivative (named 4d [**Table 5.2**]) was the best candidate in terms of EC_{50} and chemical tractability. The binding mode to RAD51 of both enantiomers of 4d, as obtained by induced-fit docking simulations, displays some points of interaction similar to those of the crystallographic BRC4-RAD51 complex. To improve the RAD51-BRCA2 inhibitory activity of 4d, researchers conducted a chemical modification campaign around the dihydroquinolone pyrazoline core in order to synthetize more efficient Zone II disruptors. This new series of dihydroquinolone pyrazoline molecules showed interesting results in the Elisa assays, with values ranging from 0.95 to 20 μM.

5.1.2.1 Preliminary selection of Zone II disruptors

To investigate the mechanism of action of the new compounds, different biological assays were performed. Our preliminary screening consisted of verifying the efficacy of compounds in inhibiting cell HR and/or in increasing the antiproliferative effect of OLA. For each compound, both parameters were verified using only one or two doses, in the range of the EC_{50} obtained with the ELISA test. HR activity was assessed by evaluating the recombination rate between two transfected plasmids, using a commercially available assay.
This preliminary investigation allowed us to rapidly exclude molecules showing: 1. low or no activity; 2. poor solubility in cell culture media; 3. a non-dose-dependent effect; 4. discrepancy between the data obtained in the two different screening procedures (e.g., HR inhibition not confirmed by increased OLA efficacy in the viability assay or, on the contrary, increased OLA efficacy without HR inhibition).
The data reported in **Table 5.2** show a list of the tested compounds and the results we obtained.
ARN 24089 (In the table reported as compound **35d**) was the most promising one in the HR activity test.

Table 5.2 *Preliminary Biological Screening of Compounds Showing EC_{50} on ELISA Assay Ranging from 0.95 to 20 μM. ARN 24089 (**35d**) results are highlighted.*

compd	EC_{50} ELISA (μM)	preliminary biological screening
4d	16 ± 4	HR inhibition = 10%, 40 μM
12d	16 ± 2	HR inhibition = not present
		olaparib association = not present
18d	13 ± 1	olaparib association = not present
20d	20 ± 2	olaparib association = not present
21d	20 ± 4	NE[a]
22d	2 ± 0.5	HR inhibition = not present
		olaparib association = not present at 5 μM
23d	10 ± 2	olaparib association = not present
30d	15 ± 3	NE[a]
31d	17 ± 4	HR inhibition = NDD[b]
		olaparib association = present at 20 μM
33d	8 ± 2	HR inhibition = not present
		olaparib association = not present
34d	19 ± 1	HR inhibition = not present
		olaparib association = NE[a]
35d	19 ± 1	HR inhibition = 54%, 20 μM
		olaparib association = present at 15 μM
36d	10 ± 0.7	HR inhibition = 24%, 10 μM
		olaparib association = not present
39d	15 ± 4	HR inhibition = NDD[b]
45d	18 ± 1	HR inhibition = not present
49d	0.95 ± 0.05	HR inhibition = not present
		olaparib association = not present

[a]**NE:** *Not Evaluable*, [b]**NDD:** *Not Dose Dependent*

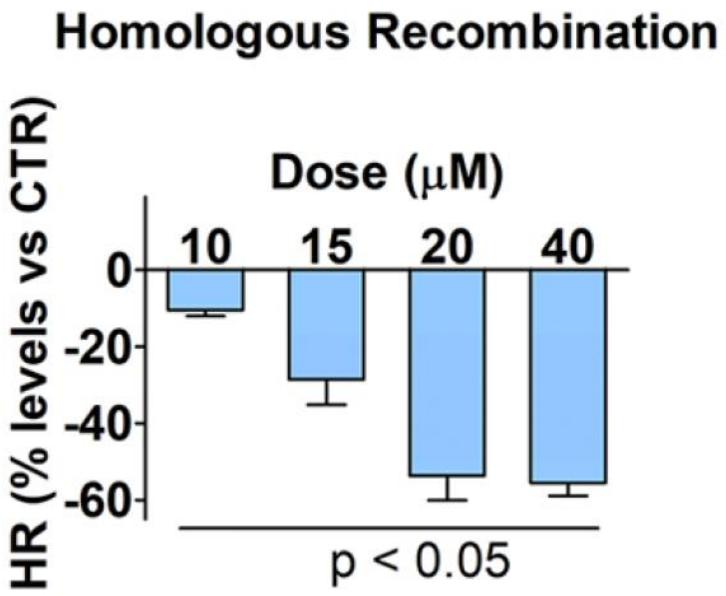

Figure 5.5 *Effect on HR caused by ARN 24089 administered to BxPC3 cells during plasmid transfection (5 h). The observed inhibitory effect was significantly different from 0 (the level of untreated cultures) for all tested doses, with $p < 0.05$.*

To further characterize the effect of ARN 24089 on HR, the compound was administered at different doses to BxPC3 cells for 5 h simultaneously with plasmid transfection. ARN 24089 produced a statistically significant dose−response effect in reducing cell HR. The compound was tested up to 40 μM (an upper limit in terms of solubility), and we estimated the dose causing a 50% inhibition of HR by applying the polynomial regression to the collected data. The EC50 was 18.4μM [**Figure 5.5**].

5.1.2.2 Immunohistochemical staining of RAD51 and γ-H2AX nuclear foci

An additional evidence of compromised HR was obtained by assessing the localization of RAD51 in BxPC-3 nuclei after DNA damage. To obtain massive DNA damage, BxPC-3 cultures were exposed for 1 h to 50 μM cisplatin (CPL). The immunohistochemical staining of RAD51 revealed evident nuclear foci in CPL-treated cells, which appeared significantly reduced when the drug was administered in association with 20 μM ARN 24089. Furthermore, the percentage of RAD51-labeled nuclei measured in cultures exposed to 20 μM ARN 24089 was superimposable to that observed in cells exposed to the association of cisplatin with 20 μM ARN 24089 [**Figure 5.6**].

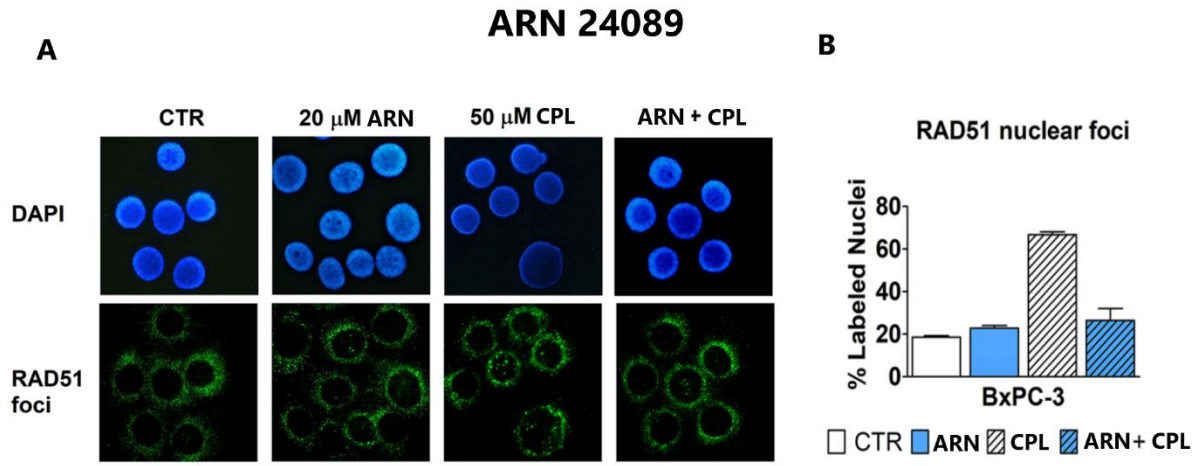

Figure 5.6. *Immunofluorescence detection of RAD51 in BxPC-3 nuclei after a treatment with 50 μM cisplatin (CPL) given separately or in combination with 20 μM ARN 24089. (A) Representative pictures showing DAPI-stained cell nuclei and the corresponding immuno-labeling of RAD51localization. In untreated cells (CTR), RAD51 labeling is clearly evident in cytoplasm and does not appear in cell nuclei. In the pictures of CPL-exposed cells, nuclear localization of the protein is clearly evident in 3 out of the 6 shown nuclei. (B) The bar graph shows the percentage of RAD51-labeled nuclei counted by two independent observers who analyzed the treated cultures. Data were statistically evaluated by applying the one-way ANOVA, which indicated a significantly increased nuclear RAD51 labeling caused by CPL ($p < 0.05$) and no statistically significant difference between cells treated with ARN 24089 and those exposed to the combination.*

The sustained inhibition of HR in cells should result in increased DNA damage, ultimately leading to mutations and chromosome aberrations; these effects are expected to be further amplified by PARP inhibition. The extent of DNA damage produced in cells treated for 48 h with 20 μM ARN 24089, administered singularly or in association with 10 μM OLA, was studied

by evidencing nuclear γ-H2AX foci by immunofluorescence. The experiment was performed on both BxPC-3 and Capan-1 cultures.
The microscope pictures showed increased evidence of γ-H2AX labeling in nuclei of BxPC-3 cells exposed to the compounds' association, compared to the labeling observed in cultures treated with OLA. In Capan-1 cultures, the constitutive γ-H2AX labeling in nuclei appeared more evident than that observed in BxPC-3 cells. Moreover, in agreement with data showing higher PARP inhibitor sensitivity for cells lacking functional HR, these cultures showed increased nuclear labeling when exposed to OLA. Notably, this labeling was not further enhanced by ARN 24089 co-administration [**Figure 5.7**].

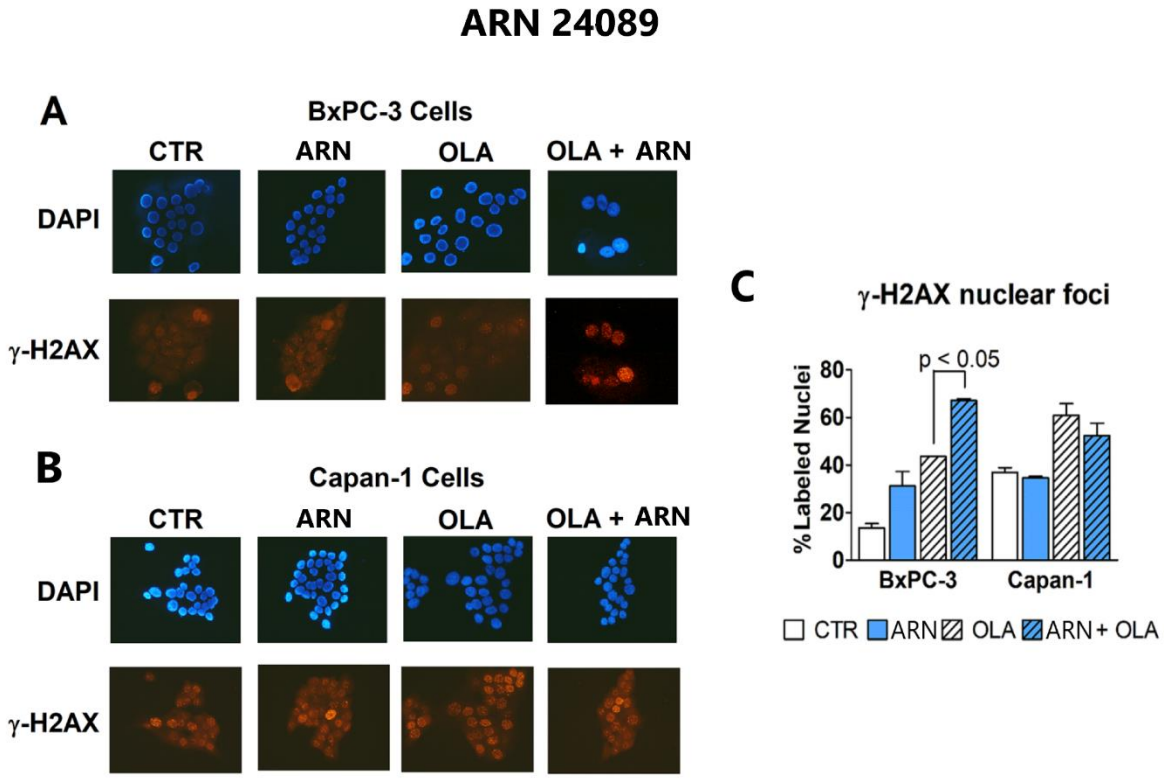

Figure 5.7. *Evaluation of DNA damage through immuno detection of nuclear γ-H2AX foci in BxPC-3 and Capan-1 cells exposed for 48 h to OLA (10 μM) or ARN 24089 (20 μM), given alone or in combination. A. DAPI-stained BxPC-3 cell nuclei and the corresponding immuno-labeling of γ-H2AX. Co-administration of ARN 24089 and OLA produced increased γ-H2AX labeling. B. DAPI-stained Capan-1 cell nuclei and the corresponding immuno-labeling of γ-H2AX. As expected, Capan-1 cells showed a constitutive γ-H2AX labeling that was highly increased by OLA but was unaffected by ARN 24089 co-administration. C. The bar graph shows the percentage of γ-H2AX -labeled nuclei counted by two independent observers who analyzed the treated cultures. Data obtained in bxPC-3 cells were statistically evaluated by applying the one-way ANOVA, which indicated a statistically significant difference between the cultures treated with olaparib and those exposed to OLA+ARN 24089 ($p<0.05$).*

5.1.2.3 Micronuclei visualization in BxPC3 treated cells

The sustained and increased DNA damage produced in BxPC-3 nuclei generates chromosomal aberrations which can be visualized through the presence of small DNA-staining bodies outside the main nucleus (micronuclei). The microscope pictures show the appearance of this feature in

BxPC3 cells exposed for 72 h to 20 μM ARN 24089, administered alone or in combination with 10 μM OLA. Notably, cells bearing micronuclei were markedly more frequent in cultures treated with the ARN 24089+OLA combination. Taken together, the results significantly support the requested mechanism of action for ARN 24089. Therefore, we conducted further experiments to test whether their combination would induce synthetic lethality. [**Figure 5.8**].

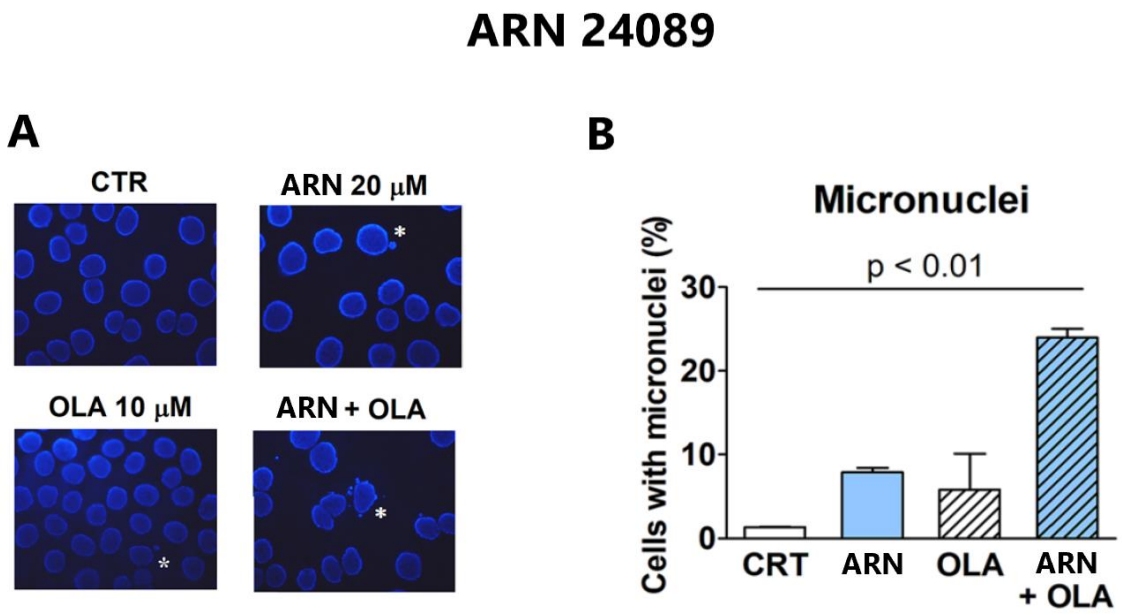

Figure 5.8. *Evaluation of micronuclei generation in BxPC3 cells treated (72 h) with ARN 24089 and OLA, given alone or in combination. A. Representative pictures showing DAPI-stained cell nuclei. White asterisks indicate the presence of micronuclei. B. The percentage of cells bearing micronuclei was estimated by two independent observers, by analyzing 100−250 cells for each treatment sample. The obtained results were statistically analyzed by applying the one-way ANOVA, which indicated a p value of <0.01.*

5.1.2.4 Cell death evaluation in ARN 24089+OLA associations

We simultaneously evaluated cell viability and cell death, measured at 72 h in BxPC3 cells exposed to ARN 24089 alone or in combination with 10 μM OLA. The statistical analysis compared the results for cultures treated with different doses of ARN 24089 or the ARN 24089+OLA combination. When applied to the data of the cell viability experiment, this analysis indicated a statistically significant difference produced by ARN 24089 in combination with OLA in all the treated BxPC3 cultures, with p values ranging from 0.01 (10 μM ARN 24089) to 0.0001 (15 and 20 μM ARN 24089) [**Figure 5.9, A**]. When we applied the same analysis to the data of the cell death experiment, we found no statistically significant increase in cell death for OLA when co-administered with 10−15 μM ARN 24089. Conversely, in cultures exposed to OLA + 20 μM ARN 24089 (the concentration that produced the highest HR inhibition in the previous experiments) the evidence for cell death was markedly increased and statistically significant, with $p < 0.0001$ [**Figure 5.9, B**].

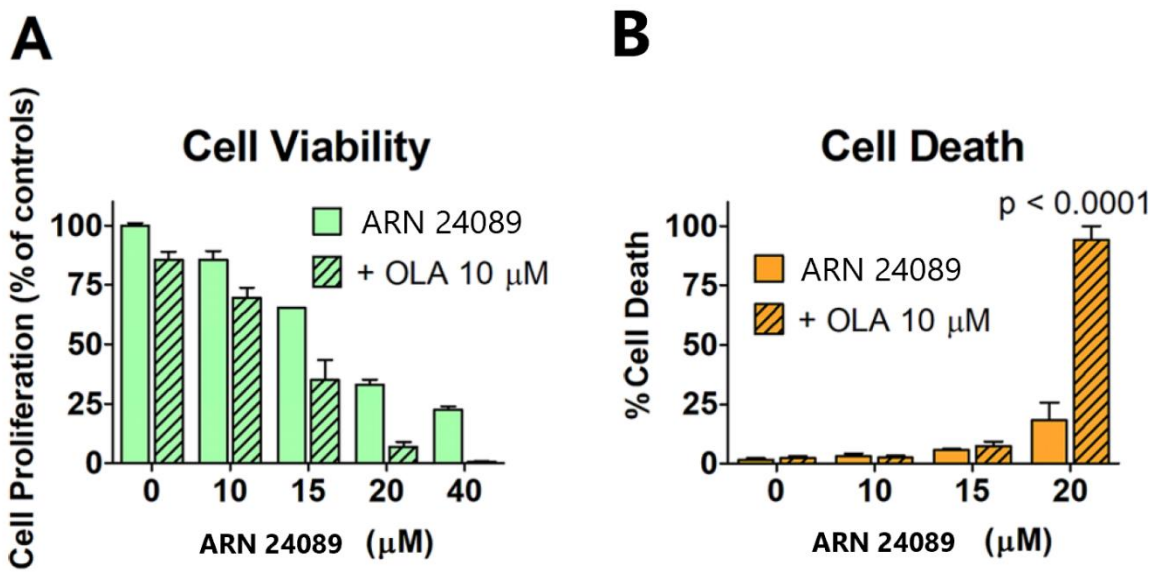

Figure 5.9. *BxPC3 cell viability (A) and death (B) measured after 72 h exposure to ARN 24089 and 10 μM OLA, given alone or in combination. Data were analyzed by two-way ANOVA using the two treatments as variables. In the cell viability experiment, Bonferroni post-test indicated a statistically significant difference produced by OLA co-administration in all BxPC3 cultures treated with the different ARN 24089 doses, with p values ranging from 0.01 (10 μM) to 0.0001 (15 and 20 μM). The same analysis was applied to the data from the cell death experiment and indicated that no statistically significant increase in cell death was produced by OLA when co-administered with 10−15 μM ARN 24089. In cultures exposed to OLA + 20 μM ARN 24089 the evidence for cell death was markedly increased and statistically significant, with p < 0.0001.*

When cell death is a consequence of progressive DNA damage accumulation induced by simultaneous PARP and HR inhibition, we would expect it to emerge gradually over time.
To confirm and better characterize the lethality observed in cultures treated with the compounds combination, we therefore considered it inappropriate to conduct a simple evaluation of the commonly used markers (e.g., caspase activation), since these can show very transient changes.
Instead, we observed cell morphology and reaction to vital dyes after the 72 h treatment: BxPC3 cells were stained with mixed DAPI and PI. The simultaneous use of these two dyes can demonstrate cell death and indicate the death pattern: DAPI is cell-permeable and shows nuclear morphology; healthy cells appear to display normal nuclear morphology in the absence of PI staining, since this dye is not cell-permeable. Cells undergoing apoptosis display nuclear condensation, which is indicated by increased DAPI staining. PI staining indicates compromised membrane integrity, which characterizes necrotic cells and late-apoptotic cells maintained in culture.
The microscope pictures show that untreated BxPC3 cells display only a moderate DAPI staining of their nucleus. Nuclear DAPI staining is slightly increased in cells treated with ARN 24089 alone but is strikingly bright only in cells treated with the ARN 24089+OLA combination. Furthermore, PI staining appeared only in these cultures, confirming the manifestation of synthetic lethality. The simultaneous marked staining of these cells with both dyes could indicate an apoptotic phenomenon followed by compromised membrane integrity because of cell persistence in culture.

As expected, the sustained and increased DNA damage observed in BxPC3 cells treated with the combination reproduced the desired mechanism of synthetic lethality. These results are also relevant given the mutated p53 status of BxPC3 cells, which should make them more resistant to mechanisms that induce cell death. [**Figure 5.10**].

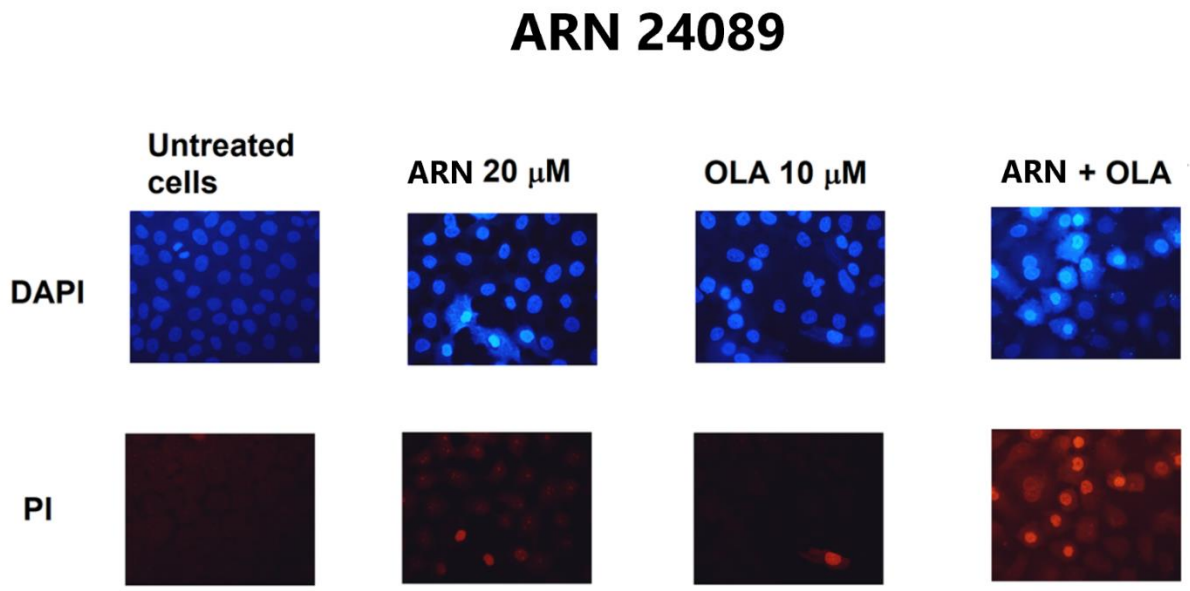

Figure 5.10. *After the 72 h treatment, BxPC3 cells were stained with vital dyes. As shown in the microscope pictures, the only culture displaying sharp evidence of cell death was that exposed to the combination of OLA+20 μM ARN 24089, as demonstrated by PI nuclear staining.*

5.1.2.5 Viability Assay with Capan-1 and HK-2

Finally, the antiproliferative effect of the ARN 24089+OLA combination was also studied on the HR- defective Capan-1 culture and on a non-neoplastic cell line derived from human kidney (HK-2). Moreover, to evaluate the antineoplastic potency of the ARN 24089+OLA association, we also calculated the combination index (CI) of the two compounds, using the procedure previously described in section **5.1.1.3**. This evaluation was performed for all the three studied cell cultures: for BxPC-3 cells, the data reported in section **5.1.2.1** were used for the calculation of CI. Interestingly, in these cells the potency of the compound combination increased in parallel with the ARN 24089 dose, reaching a statistically significant difference from 0.8 at the 20 μM concentration. The effects observed when 20 μM ARN 24089 is combined with 10 μM OLA may thus indicate a synergism between the two compounds.
In HK-2 cultures, no dose of ARN 24089 appeared to significantly increase the antiproliferative power of OLA (two-way ANOVA). In Capan-1 cells, the same statistical evaluation showed significantly increased antiproliferative effects for ARN 24089+OLA. However, in these cells, the CI did not show increasing potency of the compound combination with dose escalation. Moreover, at all tested doses, the value of CI was not significantly different from 1, which is the level measured in BxPC3 cells exposed to 10 μM ARN 24089, a dose that did not relevantly affect (≈10%) HR. This result further supports the idea that the over additive effects in the ARN 24089+OLA combination arise from and are strictly related to HR inhibition [**Figure 5.11**].

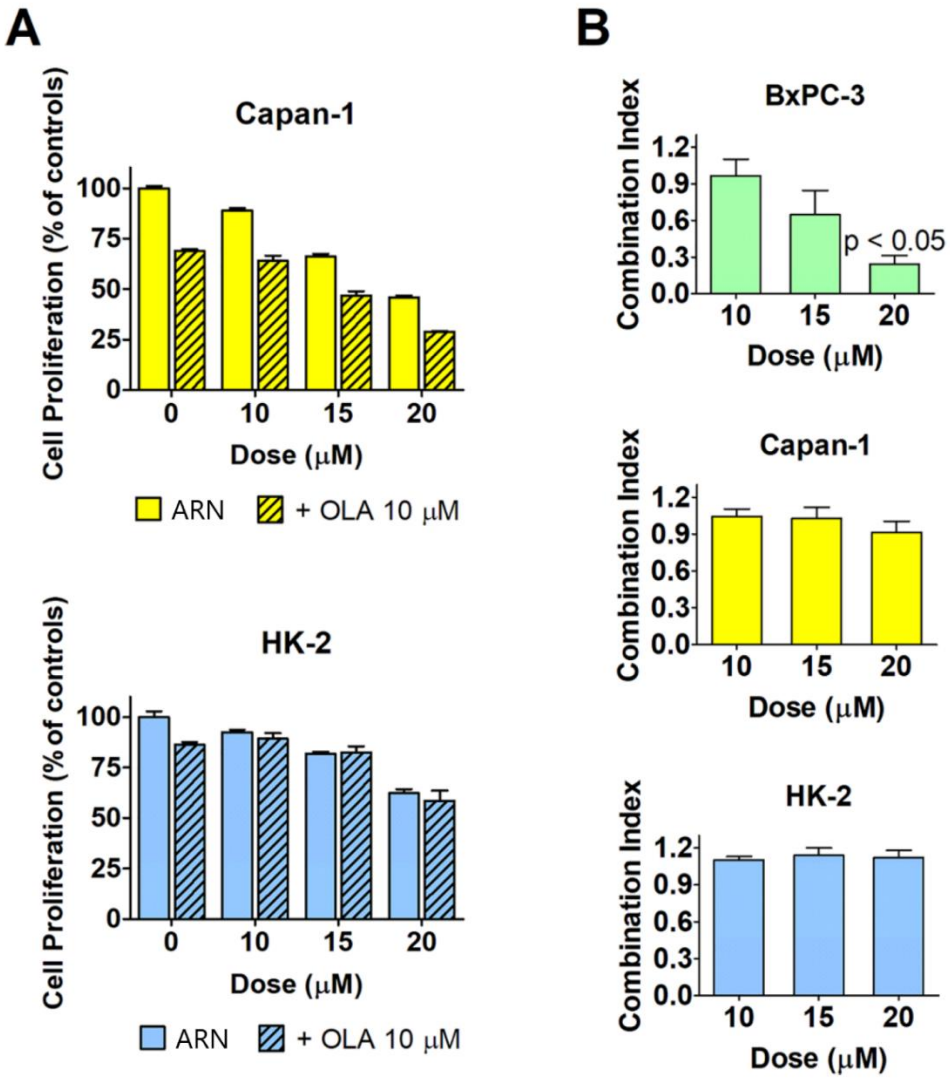

Figure 5.11. *(A) Antiproliferative effect caused by ARN 24089 and its association with OLA, measured in Capan-1 cells (RAD51-BRCA2-dependent HR does not work in these cells) and in normal immortalized human renal cells (HK-2). The same procedures described for BxPC3 cells were used here. (B) Combination indexes of the ARN 24089+OLA association measured in the three used cell lines, calculated according to the method previously described. For BxPC-3 cells, the data reported in the previous viability experiments were used. Data were analyzed using the column statistics and the one-sample t test of Prism 5 software. For BxPC-3 cells, this test showed a statistically significant difference from 0.8 for the combination of OLA and 20 μM ARN 24089. Values of <0.8 indicate synergism between the two compounds.*

Within this project, our results proved that ARN 24089 synergizes with OLA in pancreatic cancer cells (BxPC3) and can reproduce the paradigm of synthetic lethality in combination. These effects were strictly related to the extent of HR inhibition in a dose-dependent trend. This is the most promising achievement of the current investigation and supports our working hypothesis that synthetic lethality can be triggered using only small organic molecules.

5.1.2.6 Project A final discussion (Zone II disruptors)

The DNA repair and DNA damage response (DDR) pathways are suitable for the application of synthetic lethality as a novel anticancer therapeutic strategy. The classic example is the clinical application of PARP inhibitors in oncology patients with BRCA1/2 mutations. In this project, we proposed a new working hypothesis, dubbed "fully small-molecules-induced synthetic lethality". This concept combines RAD51-BRCA2 disruptors with OLA in order to simultaneously impair two DNA repair pathways and trigger the synthetic lethality mechanism.

Continuing our research line, we described a series of zone II RAD51-BRCA2 disruptors and ARN 24089 proved to be the most promising one out of all the tested compounds. ARN 24089 bound to its target (RAD51) and inhibited the protein−protein interaction between RAD51 and BRCA2. Importantly, it synergized and reproduced the paradigm of synthetic lethality in combination with OLA in pancreatic cancer cells (BxPC3). These effects were strictly related to the extent of HR inhibition in a dose-dependent trend. These results prove that it is possible to trigger synthetic lethality using only small organic molecules.

We note, however, that ARN 24089's low solubility may affect its metabolic and pharmacokinetic profile, preventing it from being studied further in in vivo cancer models. Structural tuning is therefore required (and currently ongoing) to discover more drug-like efficient zone 2 disruptors.

Interestingly, the observed synthetic lethality was triggered by tackling two biochemically different mechanisms: enzyme inhibition (PARP) and protein-protein disruption (RAD51-BRCA2). This highlights how complex and diverse mechanisms of action can synergistically contribute to the same physiological and, in turn, pharmacological activity.

In conclusion, we have further shown that synthetic lethality may be a suitable framework for discovering innovative anticancer therapies. We are confident that this novel concept will open up several new avenues based on other lethal gene pairs to meet the medical needs in oncology.

5.2 PROJECT B: INHIBITION OF HR ACTIVITY THROUGH THE USE OF LDH INHIBITORS

5.2.1 Metabolic characterization of cell cultures

Neoplastic cells typically show highly increased rates of glucose uptake and glycolysis, after which the obtained pyruvate is converted to lactate by lactate dehydrogenase (LDH). The enhanced glucose metabolism was also found to promote other cancer-essential functions. Among these, the maintenance of a certain level of DNA integrity is a crucial function for supporting active proliferation. In literature, elevation of glycolysis was found to facilitate DNA repair and to confer cancer cells resistance to ionizing radiation. Considerable amounts of evidences also suggest that inhibition of glycolysis leads to compromised DNA repair, which is accompanied by energy depletion. Furthermore, increasing evidences suggest for lactate a role as signaling factor, involved in the modulation of gene expression.

Based on the above exposed premises, the experiments reported in **Project B** were aimed at exploring a possible direct role of LDH in the DNA damage response (DDR). To do that, we used two different cell lines (named SW620 and BxPC3) who relied differently on LDH activity.

To characterize the metabolic assets of SW620 and BxPC-3 cells we evaluated the expression of the two LDH isoforms (LDH-A and -B); furthermore, we assessed the levels of lactate and ATP in cultures exposed to oxamate (OXA), a well-studied LDH inhibitor, active in the millimolar range.

The first experiment showed the relative levels of LDH-A and -B measured in the two cultures, normalized on the LDH-A expression of SW620 cells. Both cultures showed a clear prevalence of the B isoform of the enzyme [**Figure 5.12, A**]. The rate of lactate production measured in BxPC3 cells was 4-fold higher than that measured in SW620 cultures. Moreover, their ATP content dropped to a very low level when exposed to OXA, given at a dose as low as 10 mM. Opposite to BxPC-3 cultures, SW620 cells mainly base their energy metabolism on oxidative reactions since they appeared to maintain not significantly modified ATP levels even in the presence of 40 mM OXA, a dose which almost completely abolished lactate production [**Figure 5.12, B-C**]. Contrary to the current opinion linking LDH-A to actively glycolytic metabolism [75], BxPC-3 cultures, in which the -A isoform of the enzyme was undetectable, showed an energy metabolism highly dependent on glycolytic reactions and resulted extremely susceptible to OXA.

5.2.2 Cellular viability Assessed by CellTiter-Glo and Neutral Red

The two different metabolic assets of these cell cultures were also confirmed by studying the effect of OXA on cells viability, assessed after a 24 h treatment by using two different procedures: Neutral Red assay (which gives an estimate of cell number) and CellTiter-Glo Assay (which measures ATP levels).

Results showed that in SW620 cells the two procedures give superimposable results, and confirmed that energy metabolism and viability of these cells are unaffected by LDH inhibition,

at 24 h. In these cultures, the ratio ATP / cell number was unchanged for all tested doses of OXA [**Figure 5.13, B-C**].

When performed on BxPC-3 cultures, the same experiments showed that although LDH inhibition significantly affected the energy metabolism of these cells, no significantly reduction of viability was produced by 10-20 mM OXA. It is worth notice that, although viable, these cultures showed ATP levels reduced up to 30% [**Figure 5.13, A-C**].

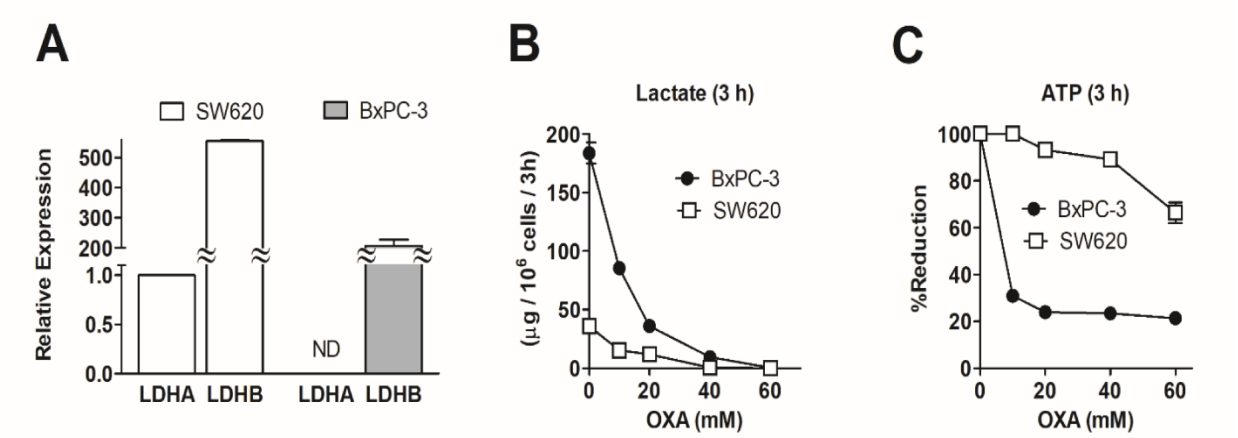

Figure 5.12. *(A) Evaluation of LDH-A and -B expression by real-time PCR. ND, not detectable. (B) Lactate and (C) ATP levels measured in BxPC-3 and SW620 cells exposed to OXA.*

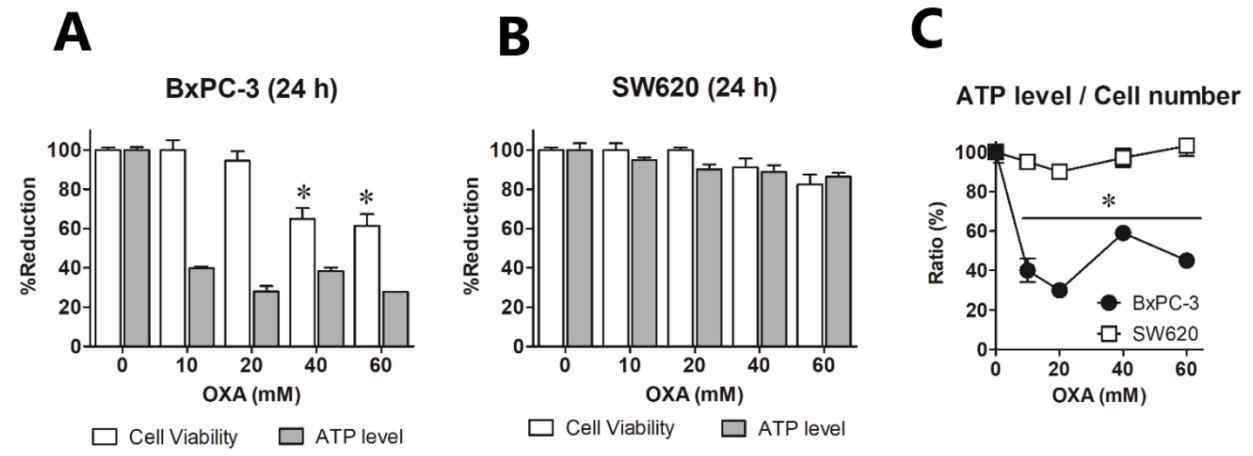

Figure 5.13. *Effect of OXA (10 mM-20 mM-40 mM-60 mM) on the viability of BxPC3(A) and SW620(B) cultures after 24h of treatment, assessed through the measure of ATP level or by evaluating cell number. In the case of BxPC-3 cells, the two procedures gave different results; when cell viability was assessed by evaluating cell number, no statistically significant effect appeared to be produced by 10 and 20 mM OXA at 24 h. Viability data were analyzed were analyzed by one-way ANOVA followed by Dunnet 's post-test. *, p < 0.01 compared to control cultures. (C) Ratio ATP level / cell number, calculated from the results shown in (D,E). Data were analyzed one-way ANOVA followed by Dunnet's post-test. (*) p < 0.01 compared to control cultures. For further explanation, see text.*

5.2.3 Study of homologous recombination in LDH-inhibited cells

Both cultures were exposed to OXA given for 16 h at a dose causing significant inhibition of LDH enzymatic activity without affecting cell viability: 10-20 mM OXA was used for BxPC-3; 40 mM for SW620 cultures. To test HR function in OXA-exposed cultures, we assessed:

1. expression of genes involved in HR repair,
2. plasmid recombination in transfected cells,
3. extent of DNA damage caused by OLA,
4. nuclear localization of RAD51 induced by a DNA damaging agent.

5.2.3.1 Expression level of HR-related genes

The expression level of a panel of genes was assessed by real-time PCR: BRCA1 and -2, RAD51 and other genes involved in the HR mechanism (MRE11A; RAD50; NBN). Predictably, in ATP-depleted BxPC-3 cells the expression of all examined genes appeared significantly lowered, with a variation ranging from -22% (BRCA1) to -50% (NBN) [**Figure 5.14, A (white bars)**].
However, a statistically significant reduced expression of the same gene panel was also observed in SW620 cells, in which even higher effects were observed (-72% for BRCA2; -46% for RAD51) [**Figure 5.14, B (white bars)**].
Studies report that the product of LDH reaction (lactate) has an impact on histone acetylation and gene expression [89-90]. For this reason, and in search of a possible explanation to the results observed in SW620 cells, we exposed these cultures to the same OXA treatment supplemented with 10 mM lactate. In line with published data, lactate supplementation was found to significantly reverse most of the changes observed in SW620 cells [**Figure 5.14, B (dark bars)**].
Unexpectedly, in spite of their ATP-lowered content, BxPC-3 cells were more responsive to the effects of this metabolite [**Figure 5.14, A (dark bars)**].
Taken together, the results suggest that LDH activity could be involved in controlling the expression of a crucial group of genes involved in HR. Depending on the cell context, the role of this enzyme in maintaining energy balance can contribute in causing the downregulated gene expression. However, a major impact appears to derive from the non-metabolic functions of the LDH reaction product.

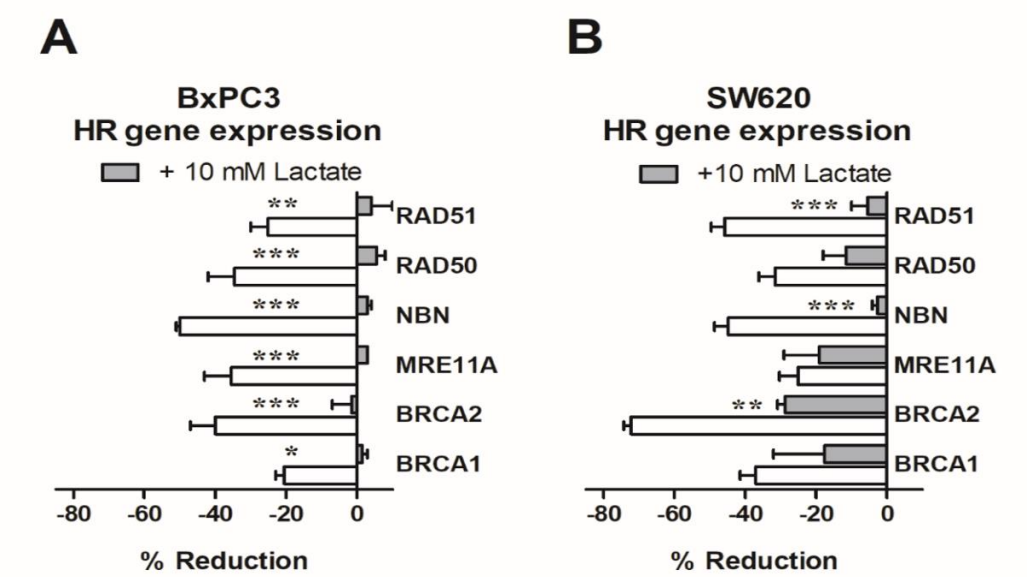

Figure 5.14. *A group of key genes involved in the HR pathway was examined by real-time PCR in BxPC-3 (A) and SW620 cultures (B) exposed for 16 h to OXA. Data were evaluated using one-way ANOVA followed by Dunnet's post-test. In BxPC-3 cells, a statistically significant reduced expression was found for all examined genes, with the exception of BRCA1; p values ranged from <0.05 to <0.01. In the case of SW620 cells, a statistically significant difference compared to control cultures was observed for all genes, with p<0.01. The graphs also show the effect of lactate supplementation on gene expression (grey bars). In spite of their ATP-lowered content, BxPC-3 cells proved to be very responsive to this metabolite, which completely reversed all the OXA-driven effects. In SW620 cells lactate was able to significantly reverse the effects of LDH inhibition in 3 out of 6 genes. (*), p < 0.05; (**) < 0.01 (**); (***) < 0.001.*

5.2.3.2 Evaluation of plasmid recombination in OXA treated cells

We applied to OXA-exposed cultures a commercially available assay specifically designed to study the co-transformation in bacterial cells of two plasmids bearing homology sequences. The provided couple of plasmids can be also transfected into mammalian cells. In these cells, they recombinate in episomal form using the enzymatic machinery of the host and produce a real-time PCR detectable sequence. In line with the results of the previous experiments, in BxPC-3 cells the obtained recombination product appeared to be significantly decreased. On the contrary, in SW620 cultures higher rates of plasmid recombination were detected [**Figure 5.15**].

To explain this finding, we hypothesized that in these cultures alternative pathways of DNA recombination can take place when HR genes are down regulated. These pathways have also been described as more rapid and, consequently, more error prone when compared to HR.

We measured the expression of a list of genes involved in alternative recombination pathways: classical non-homologous end joining (NHEJ) and alternative end joining (EJ). The expression of these genes was examined in both the OXA-treated cultures. Predictably, in ATP depleted BxPC-3 cells 5 out of 10 examined genes involved in NHEJ and/or alternative EJ were found to be downregulated. On the contrary, in SW620 cells a reduced expression was detected only in two genes, suggesting that in these cultures the alternative pathways could work and their prompt activity should allow rapid recombination events [**Table 5.3**].

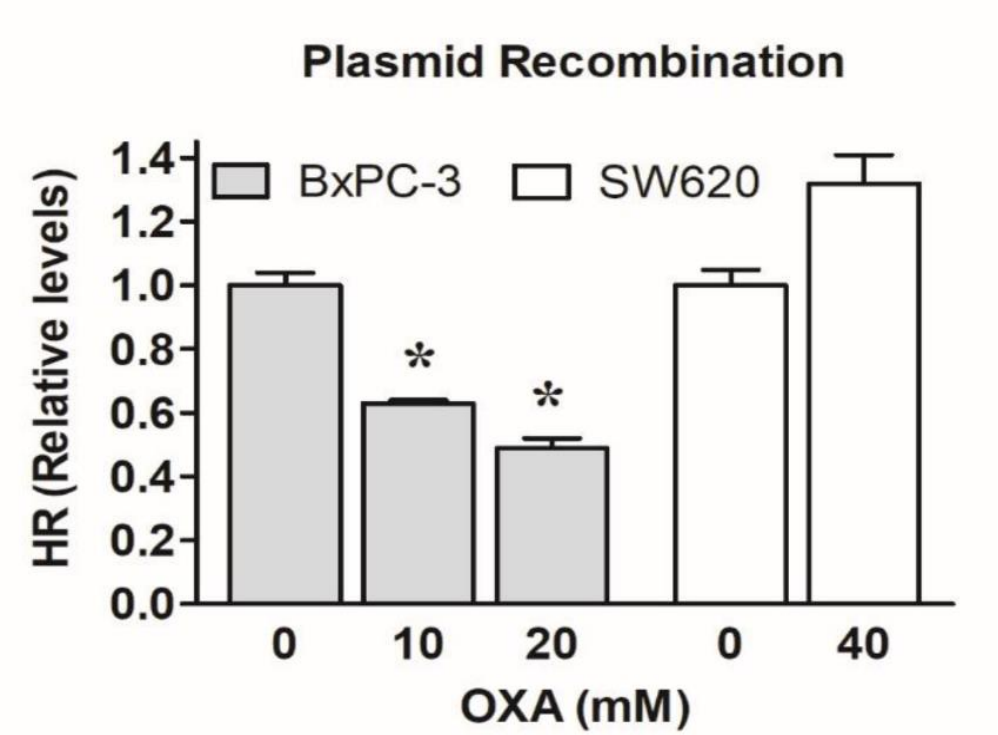

Figure 5.15. *Episomal plasmid recombination assessed in the two cell lines by using a commercially available assay. For explanation, see text. In BxPC-3 cells, a statistically significant reduction was observed for both OXA doses, with $p < 0.05$ (*) (ANOVA).*

Table 5.3. *Expression of genes involved in alternative pathways to homologous recombination repair. Changes observed in cells exposed to OXA.*

Gene	Protein	DDR Pathway	% Variation in BxPC3 cells	% Variation in SW620 cells
DCLRE1C	Artemis	Classical NHEJ	ND*	ND
LIG4	Ligase 4		- 21 ± 9	ND
PRKDC	DNAPKcs		ND	ND
XRCC4	XRCC4		- 38 ± 7	- 34 ± 3
XRCC5	Ku80		- 46 ± 6	ND
XRCC6	Ku70		- 48 ± 8	ND
LIG1	Ligase 1	Alternative EJ	ND	- 38 ± 4
PARP1	PARP		-30 ± 2	ND
WRN	Werner helicase		ND	ND
XRCC1	XRCC1		ND	ND

* ND, not detected. Only changes exceeding 20% have been considered.

5.2.3.3 γ-H2AX immunoblotting in OXA/OLA treated cells

For this experiment, cells were exposed for 16 h to OXA administered singularly or in association with OLA (10 μM). This OLA dose was chosen on the basis of results obtained by studying the association of OLA with different inhibitors of HR (**Project A**). As well documented, in conditions of compromised HR repair (e.g. in BRCA1/2 defective cancer cells) PARP inhibition results in increased DNA damage signatures, which can be evaluated by assessing γ-H2AX levels, a commonly used DNA damage indicator. This effect was entirely reproduced in SW620 cells exposed to the association of the two compounds. In these cultures, OLA caused enhanced γ-H2AX levels, but the simultaneous exposure to OXA was found to significantly increase the effects of PARP inhibition, giving a proof compromised HR in LDH-inhibited cells [**Figure 5.16, A**].
On the contrary, and in spite of the results obtained in the two previous assays, LDH inhibition did not appear to induce significantly increased DNA damage in OLA-exposed BxPC-3 cells. In our opinion, this result can be easily explained considering that ATP deprivation of LDH-inhibited BxPC-3 cells is expected to impact on phosphorylation-mediated signaling and to reduce cell competence in managing DNA damage [**Figure 5.16, B**].

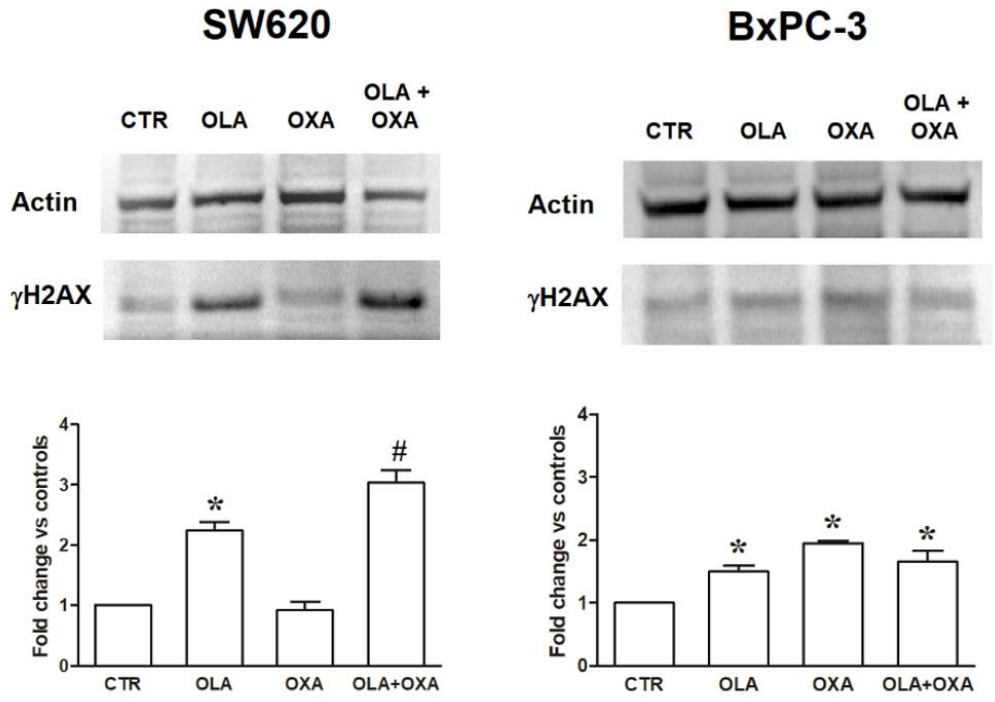

Figure 5.16. *DNA damage was assessed by an immunoblotting evaluation of H2AX histone phosphorylation (γ-H2AX). The experiment was performed in both cell cultures exposed for 16 h to OXA and 10 μM OLA, administered separately or in association. 10 and 40 mM OXA were used in BxPC-3 and SW620 cells, respectively. The bar graphs show a densitometric estimation of γH2AX bands, normalized on Actin levels. In the case of SW620 cells, OLA was found to significantly increase γH2AX level; the extent of DNA damage was further raised by the association OXA/OLA (A). In BxPC-3 cells a slight, but statistically significant increased level of γH2AX was observed in all treated samples; however, in these cells OXA did not caused increased DNA damage in OLA-exposed cultures (B). *, $p < 0.05$, compared to control cells. #, $p < 0.05$, compared to OLA treated cells (one-way ANOVA and Bonferroni's post-test).*

5.2.3.4 Evaluation of RAD51 nuclear translocation upon CPL treatment

A further proof of compromised HR in LDH-inhibited cells was obtained by studying RAD51 nuclear translocation following a short exposure to cisplatin (CPL), a chemotherapeutic agent causing direct DNA damage. BRCA2-mediated translocation of RAD51 in cell nuclei is one of the earliest events at the onset of HR repair. The nuclear localization of RAD51 can be evidenced by an immunofluorescence staining of this protein in CPL treated cells. In this experiment, CPL was found to significantly increase RAD51 immunolabeling in the nuclei of both BxPC-3 and SW620 cultures, with a p value < 0.05 and 0.01, respectively. When administered to untreated cells, OXA did not modify the nuclear immunolabeling of RAD51; on the contrary, when administered to CPL-probed cells, the LDH inhibitor appeared to reduce RAD51 immunolabeling in nuclei to a level not dissimilar from that of untreated cells [**Figure 5.17**].

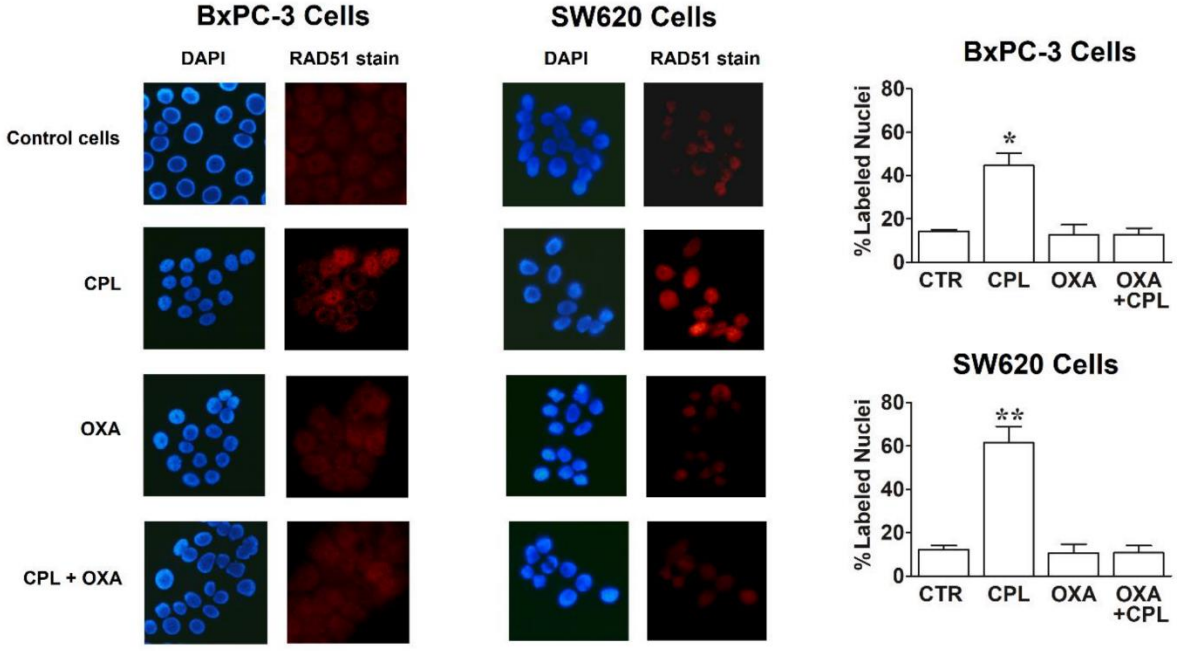

Figure 5.17. *Cell cultures were probed with 50 µM CPL for 1.5 h and maintained in the presence of OXA for 24 h. The data reported in the bar graphs were statistically evaluated by one-way ANOVA followed by Dunnet's post-test. Asterisks indicate a significant difference compared to untreated cells (CTR), with p < 0.05 (*) and p < 0.01 (**).*

Taking these data together, in both BxPC-3 and SW620 cultures three of the four applied procedures to evidence inhibited HR after LDH inhibition gave coherent results. In both cultures, we observed a single inconsistency: in OLA-exposed BxPC-3 cultures, OXA treatment did not result in increased DNA damage [**Figure 5.16, B**]. In OXA-treated SW620 cells, plasmid recombination was found to proceed at even higher rates [**Figure 5.15**]. Since both these discrepancies can be easily explained, the obtained results overall suggest that LDH inhibition reduce operative HR in both the used cell cultures, independently of their different metabolic asset.

5.2.4 Cell viability and death in combination experiments with OXA and OLA

After proving that LDH inhibition could impair HR, we wanted to verify if it could also increase the effect of OLA in BRCA-proficient cells. We performed various combination experiments with OXA and OLA, aimed at assessing cell viability and death caused by the compounds' association. The obtained data were statistically evaluated by two-way ANOVA using the OLA doses and OXA supplementation as variables.
In BxPC-3 cells, the potency of the compounds' association increased in parallel with the doses of OLA and OXA, and this effect was observed in the study of both cell viability and death. In both experiments, the statistical evaluation showed a strongly significant interaction between the two compounds, with $p < 0.0001$.

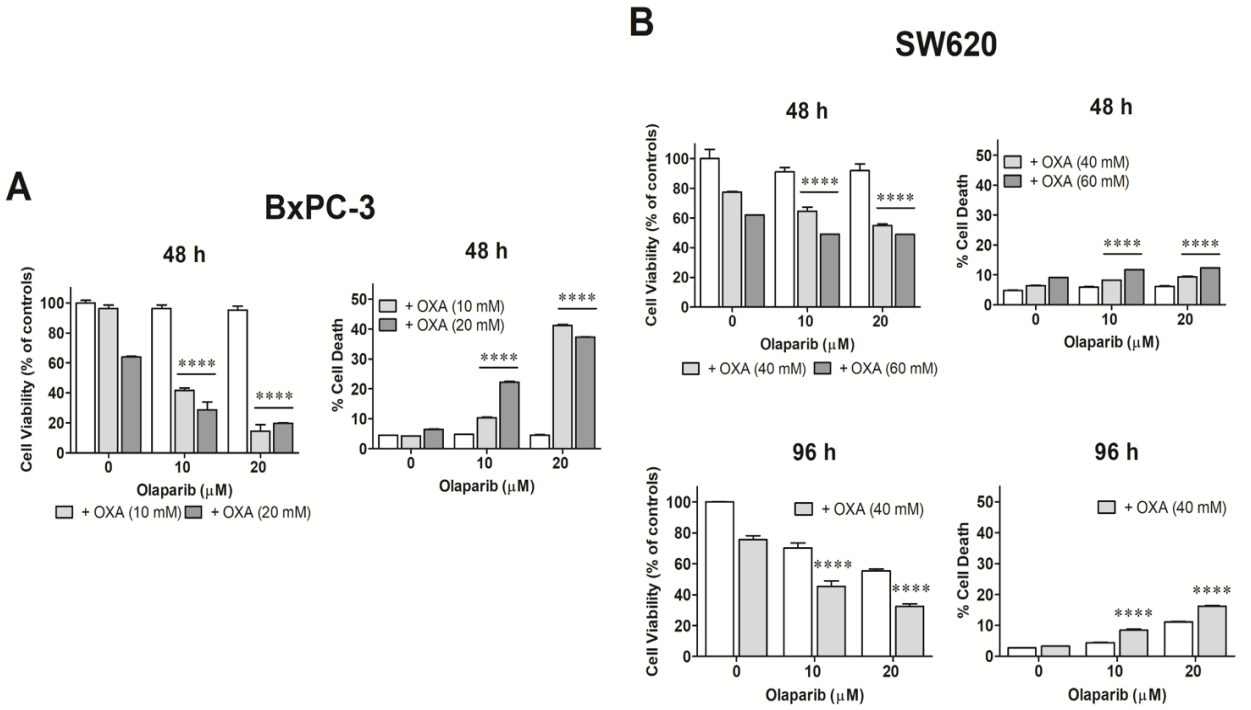

Figure 5.18. *Cell viability was studied by applying the Neutral Red assay in BxPC-3 (A) and in SW620 (B) cultures treated for the indicated time with OXA and OLA, administered singularly or in combination. Cell death was assessed by using the CellTox™ Green Cytotoxicity Assay (Promega), following the instruction of the manufacturer. Data were statistically analyzed by applying the two-way ANOVA, using OLA and OXA supplementation as variables. ****, $p < 0.0001$, when compared to OLA administered as a single treatment (Bonferroni's post-test). The viability data reported in (A) and (B) were also used for an estimation of the C.I. of the OXA/OLA association. A detailed explanation of the obtained results is given in the text.*

Interestingly, the heavily lethal effects observed in these cells at 48 h cannot be simply ascribed to the impaired energy metabolism caused by LDH inhibition, since they appeared only in cultures treated with the compounds' association [**Figure 5.18, A**].
In studying cell viability of the SW620 cultures a statistically significant effect caused by OXA and OLA was observed, both at 48 and at 96 h, with p values ranging from 0.0002 to < 0.0001. However, in this case the statistical analysis indicated no interaction between the two compounds, suggesting that, although statistically significant, the effect of OXA

supplementation is similar for both the tested doses of OLA. Although in SW620 cultures the evidence of cell death caused by the association OLA/OXA was quite lower than that observed in BxPC-3 cells, the interaction between the two compounds on this parameter resulted statistically significant, with $p = 0.039$ at 48 h and $p < 0.0001$ at 96 h [**Figure 5.18, B**].
These results suggest that the increased potency of the compounds' association is mainly evidenced when considering its lethal effects, even though the entity of these effects can variate depending on the cell context. Notably, the induction of alternative recombination pathways can be a crucial factor driving lethality in cells with inhibited HR and PARP function and, as described above, in OXA-treated SW620 cells these pathways seem to be operative.
The potency of the OXA/OLA association was also evaluated by applying to the data of cell viability the procedure to assess the combination index (CI) between an enzyme inhibitor and antineoplastic agents. This calculation procedure was already used to evaluate the potency of the association OLA / RAD51-BRCA2 disruptors [**5.1.1.3**].
When applied to the overall viability data obtained in BxPC-3 cells, this procedure returned a CI = 0.35, with a 95% confidence interval ranging from 0.12 to 0.58, clearly indicating for these cells the occurrence of synergism between the two compounds. In the case of SW620 cultures, a CI = 0.84 was measured, with a 95% confidence interval ranging from 0.77 to 0.91. Therefore, in this case the interaction between OXA and OLA appeared to be characterized by additive effects. Taken together, the results are in total agreement with the indications given by the two-way ANOVA test.

5.2.5 Cell death evaluation in combination experiments with OXA and OLA

We designed a new set of experiments aimed at better defining the cell death pattern observed in the two cell cultures. In these experiments, the two cell cultures were exposed to the OLA/OXA association for 48 h and then treated with vital dyes (DAPI and PI) without a fixation step in paraformaldehyde. The simultaneous use of these two dyes can demonstrate cell death, also giving indication on the death pattern. DAPI is cell-permeable and evidences nuclear morphology; healthy cells appear to display normal nuclear morphology in the absence of PI staining, since this dye is not cell-permeable. Cells undergoing apoptosis display nuclear condensation, which is indicated by increased DAPI staining. PI staining indicates compromised membrane integrity, which characterizes necrotic cells and late-apoptotic cells maintained in culture.
The DAPI/PI staining procedure confirmed the massive death of BxPC-3 cells already observed at 48 h in the previous set of experiments. The bright PI staining of these cultures suggest loss of membrane integrity, as can be expected in cells with compromised energy metabolism. SW620 results were also in agreement with the previously obtained data, showing a low level of cell death at 48 h [**Figure 5.19**].
For this reason, cell death was further investigated by an immunoblotting evaluation of the BAX/BCL2 ratio, which was performed in both cell lines. Although BxPC-3 and SW620 cells appeared to express different BAX and BCL2 levels, the densitometric calculation of the ratio between the two proteins showed superimposable changes in response to the applied treatments.

In both cultures, apoptosis appeared to be significantly increased (compared to control cells) only because of the combined OLA/OXA treatment. [**Figure 5.20**].
Those findings suggested that the molecular signatures of apoptosis were evident in both cell cultures at a very similar level. Furthermore, they indirectly confirmed that the reduced ATP availability of OXA-exposed BxPC-3 cells can be the key factor in generating the membrane damage and the consequent heavy lethality observed in these cultures.

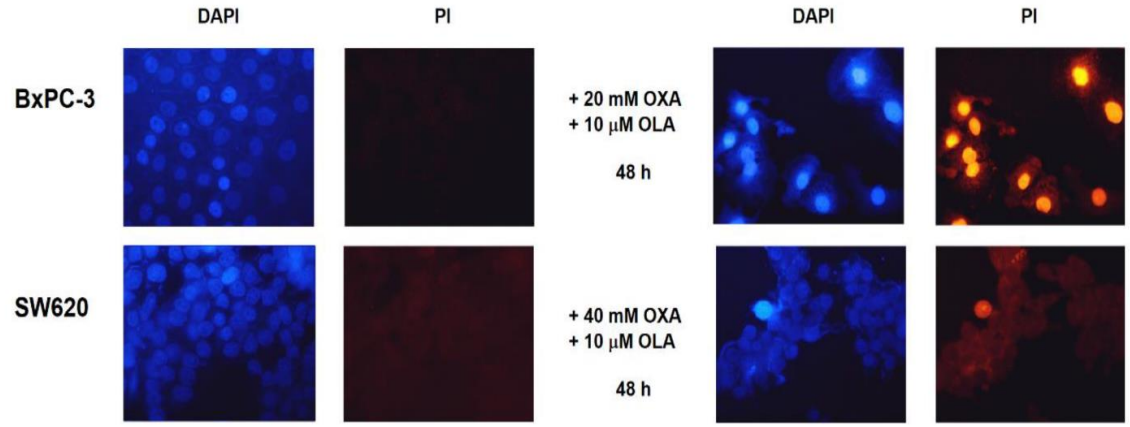

Figure 5.19. *Assessment of cell death with vital dyes. In BxPC-3 cells death appeared to be sharply evident. The observed staining pattern is compatible with apoptosis (increased DAPI staining suggesting nuclear condensation) followed by damaging of membranes (deep PI staining). In SW620 cultures PI staining pattern appeared pale and limited to some areas of the microscope slide. For this reason, an additional assay was applied to these cells.*

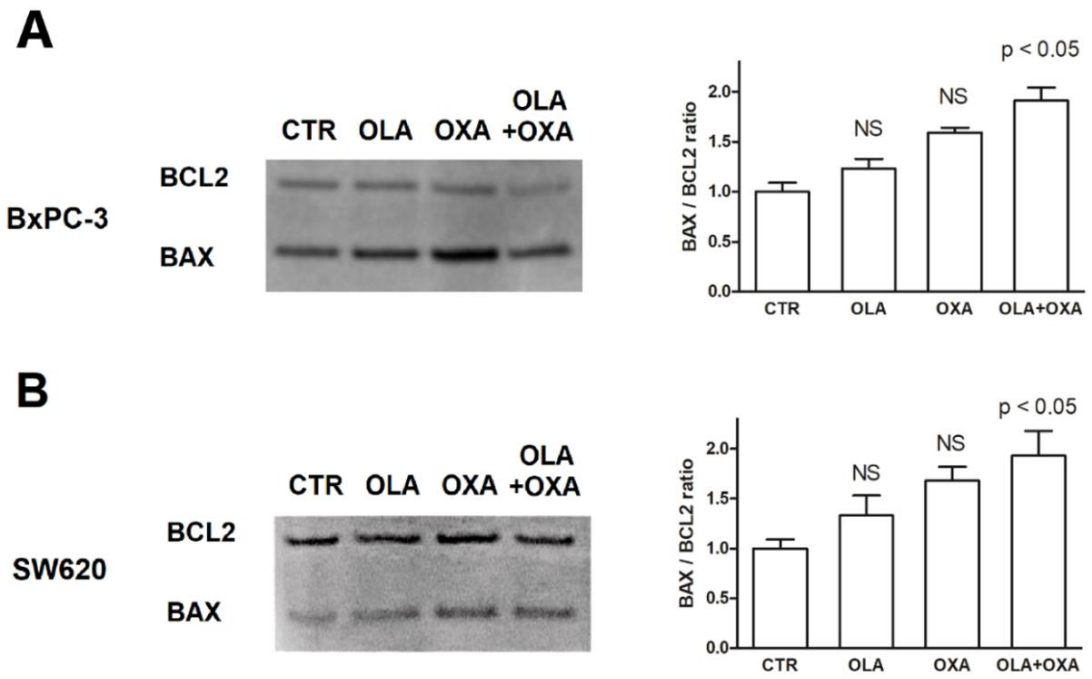

Figure 5.20. *Assessment of apoptosis at the molecular level, through the immunoblotting evaluation of BAX/BCL2 ratio in BxPC3 (A) and SW620 (B) cells. As shown in the bar graph, only cultures treated with the compounds' association showed a statistically significant difference in their BAX/BCL2 ratio when compared with untreated cells (ANOVA) NS, not significant.*

5.2.6 Project B final discussion

LDH is a major player in cancer cell metabolism. The data of our preliminary investigation suggested an LDH-mediated control on HR, the most critical DDR pathway for restoring chromosome integrity and, hence, potentially affecting cell response to chemotherapeutic agents. Our results indicate that this control could be exerted by simply assuring the adequate energy supply needed to the DDR and/or by regulating the expression level of genes involved in DNA repair. Although preliminary, they highlight a complex relationship between metabolic reactions and the control of DNA integrity. Furthermore, they offer a mechanistic explanation to several published reports showing increased cell response to antineoplastic agents after LDH inhibition or knockdown.

In latest years, in the attempt of developing innovative anticancer strategies, treatments with small molecules able to hinder DNA repair have been proposed. The rationale underlying this therapeutic approach lies in the genetic instability of cancer cells, which makes them more dependent on DNA repair mechanisms, compared to healthy cells. PARP inhibitors (e.g. OLA) are a well-known example of antineoplastic drugs targeting the DDR. However, clinical experience with these compounds showed successful therapeutic results only on cancer forms characterized by HR deficiency, which cannot compensate for the inhibited PARP function. To broaden the use of PARP inhibitors, the association of OLA with conventionally used chemotherapeutics was also proposed, with the aim to obtain enhanced therapeutic power. Furthermore, the effect of this drug was tested in cancer contexts characterized by different DNA repair deficiencies, such as colon cancer with microsatellite instability. However, these approaches were often found to produce increased systemic toxicity; in addition, the potential increased risk of incurring in secondary malignancies, after the successful control of the primary tumor should be considered.

The findings described in this thesis suggest a possible use of LDH inhibitors to extend the use of OLA to HR proficient tumor forms. Recently, the first LDH inhibitor potentially active in vivo has been identified. In the used animal model, the only observed toxic effect that could potentially narrow the therapeutic window of this novel compound was found to be hemolysis, presumably linked to the metabolic inhibition of red blood cells. Taken together, these data suggest a combination of OLA with LDH inhibitors as a worthwhile therapeutic attempt to dampen the proliferative potential of cancer cells with tolerable side effects on normal tissues.

6. CONCLUSIONS

In recent years, innovative anticancer treatments have relied on targeted therapies to improve drug efficacy and reduce side effects. The use of novel molecules or antibodies that could precisely target a single protein has increased the chances of survival of many patients.
One of these innovative treatments involves the use of small drugs to induce synthetic lethality in tumors with specific genetic mutations: the main example is the use of PARP inhibitors, such as OLA, in tumors with BRCA1/2 mutations. The effectiveness of this treatment has been demonstrated in ovarian cancer (for which OLA was originally approved), and in clinical trials in breast and pancreatic cancers.
In this project, we report a new approach to the synthetic lethality treatments dubbed "fully small-molecule induced synthetic lethality". This paradigm was based on the observation that, by using a small organic molecule capable of impairing the HR mechanism, it is possible to mimic the effect of BRCA2 germline mutations and widen the population of patients eligible for treatment with OLA and other PARP inhibitors.

In our experiments, we impaired HR mechanism using a direct and an indirect approach and we obtained meaningful results with both of them.
In **project A**, ARN 24089 could bind to its target (RAD51) and inhibit the protein−protein interaction between RAD51 and BRCA2. Importantly, it synergizes and reproduces the paradigm of synthetic lethality in combination with OLA in pancreatic cancer cells (BxPC3).
In **project B**, our data suggest an LDH-mediated control on HR, the most critical DDR pathway for restoring chromosome integrity. Although preliminary, they highlight a complex relationship between metabolic reactions and the control of DNA integrity. Furthermore, LDH inhibition also managed to increase the efficiency of OLA in all the tested cell lines and triggered the synthetic lethality mechanism.

In conclusion, these projects demonstrated that in some cases it is possible to apply an anticancer therapy (in our case, synthetic lethality therapies) to a wider type of cancers by utilizing small molecules that mimic a specific cellular environment. This could open up new possibilities for the treatment of cancers with high mortality rates, such as pancreatic adenocarcinoma, which is particularly therapy resistant.
We believe that the "fully small-molecule induced synthetic lethality" will prove to be useful even with other synthetic lethality gene pairs and will be able to meet the medical needs in the future of the oncology research fields.

7. BIBLIOGRAPHY

1. National Cancer Institute, <https://www.cancer.gov/publications/dictionaries/cancer-terms/def/cancer>.

2. World Health Organization, 12 September 2018, <https://www.who.int/news-room/fact-sheets/detail/cancer>.

3. Sawyers CL. **Chronic Myeloid Leukemia**. N Engl J Med (1999), Volume 340:1330-1340.

4. Nowell PC, Hungerford DA. **Chromosome Studies in Human Leukemia. II. Chronic Granulocytic Leukemia**. Journal of the National Cancer Institute (1961), Volume 27, Issue 5: 1013–1035

5. Druker BJ, Talpaz M, Resta DJ, Peng B, Buchdunger E, et al. **Efficacy and safety of a specific inhibitor of the BCR-ABL tyrosine kinase in chronic myeloid leukemia**. N. Engl. J. Med. (2001), Volume 344: 1031-1037.

6. Brieger J, Weidt EJ, Lindblad P, Storkel S, Huber C, Decker HJ. **Inverse regulation of vascular endothelial growth factor and VHL tumor suppressor gene in sporadic renal cell carcinomas is correlated with vascular growth: an in vivo study on 29 tumors.** J Mol Med (1999), Volume 77: 505-510.

7. Escudier B, Pluzanska A, Koralewski P, Ravaud A, Bracarda S, et al. **Bevacizumab plus interferon alfa-2a for treatment of metastatic renal cell carcinoma: a randomised, double-blind phase III trial**. The Lancet (2008), Volume 370, Issue 9605: 2103-2111.

8. Wright S, Dobzhansky T. **Genetics of natural populations. XII. Experimental reproduction of some of the changes caused by natural selection in certain populations of Drosophila pseudoobscura**. Genetics (1946), Volume 31:125-156.

9. Chin L, Tam A, Pomerantz J, et al. **Essential role for oncogenic Ras in tumour maintenance**. Nature (1999), Volume 400: 468–472.

10.Steckel M, Molina-Arcas M, Weigelt B, et al. **Determination of synthetic lethal interactions in KRAS oncogene-dependent cancer cells reveals novel therapeutic targeting strategies**. Cell Res (2012), Volume 22: 1227-1245.

11. Ruggero D. **The role of Myc-induced protein synthesis in cancer**. Cancer Res (2009) Volume 69, Issue 23: 8839–8843.

12. Pourdehnad M, Truitt ML, Siddiqi IN, Ducker GS, Shokat KM, Ruggero D. **Myc and mTOR converge on a common node in protein synthesis control that confers synthetic lethality in Myc-driven cancers**. Proc Natl Acad Sci USA (2013), Volume 110: 11988-11993.

13. Ebert BL, Pretz J, Bosco J, Chang CY, Tamayo P, Galili N, Raza A, Root DE, Attar E, Ellis SR, Golub TR. **Identification of RPS14 as a 5q- syndrome gene by RNA interference screen**. Nature (2008), Volume 451: 335-339.

14. Wei S, Chen X, Rocha K, Epling-Burnette PK, Djeu JY, Liu Q, et al. **A critical role for phosphatase haplodeficiency in the selective suppression of deletion 5q MDS by lenalidomide**. Proc Natl Acad Sci USA (2009), Volume 106: 12974-12979.

15. Morandell S, Reinhardt HC, Cannell IG, et al. **A reversible gene-targeting strategy identifies synthetic lethal interactions between MK2 and p53 in the DNA damage response in vivo**. Cell Rep (2013), Volume 5: 868-877.

16. Jiang H, Reinhardt HC, Bartkova J, et al. **The combined status of ATM and p53 link tumor development with therapeutic response**. Genes Dev (2009), Volume 23: 1895-1909.

17. Baldwin A, Grueneberg DA, Hellner K, et al. **Kinase requirements in human cells: V. Synthetic lethal interactions between p53 and the protein kinases SGK2 and PAK3**. Proc Natl Acad Sci USA (2010), Volume 107: 12463-12468.

18. Bryant HE, Schultz N, Thomas HD, et al. **Specific killing of BRCA2-deficient tumours with inhibitors of poly(ADP-ribose) polymerase**. Nature (2005), Volume 434: 913-917.

19. Herceg Z, Wang ZQ (June 2001). **"Functions of poly(ADP-ribose) polymerase (PARP) in DNA repair, genomic integrity and cell death"**. Mutation Research. (2001), Volume 477, Issues 1–2: 97–110.

20. Gradwohl G, et al. **The second zinc-finger domain of poly(ADP-ribose) polymerase determines specificity for single-stranded breaks in DNA**. Proc Natl Acad. Sci. USA (1990), Volume 87, Issue 8: 2990-2994.

21. Wei YF, et al. **Molecular cloning and expression of human cDNAs encoding a novel DNA ligase IV and DNA ligase III, an enzyme active in DNA repair and recombination**. Mol. Cell. Biol. (1995), Volume 15: 3206-3216.

22. Navas TA, Zhou Z and Elledge SJ. **DNA Polymerase ε Links the DNA Replication Machinery to the S Phase Checkpoint**. Cell (1995), Volume 80: 29-39.

23. Lindahl T, Satoh MS, Poirier GG, Klungland A. **Post-translational modification of poly (ADP-ribose) polymerase induced by DNA strand breaks**. Trends in Biochemical Sciences (1995), Volume 20, Issue 10: 405-411.

24. Henning RJ, Bourgeois M, Harbison RD. **Poly(ADP-ribose) Polymerase (PARP) and PARP Inhibitors: Mechanisms of Action and Role in Cardiovascular Disorders**. Medicine, Cardiovascular Toxicology (2018), Volume 18, pages493–506.

25. Brochu G, et al. **Mode of action of poly(ADP-ribose) glycohydrolase.** Biochimica et Biophysica Acta (1994), Volume 1219: 342-350.

26. Zahradka P, Ebisuzaki K**. A Shuttle Mechanism for DNA-Protein Interactions**. European Journal of Biochemistry (1982), Volume 127, Issue 3: 579-585.

27. Virág L. **Structure and function of poly(ADP-ribose) polymerase-1: role in oxidative stress-related pathologies**. Curr Vasc Pharmacol. (2005), Volume 3, Issue 3: 209-14.

28. Murai J, Huang SY, Das BB, Renaud A, Zhang Y, Doroshow JH, Ji J, Takeda S, Pommier Y. **Trapping of PARP1 and PARP2 by Clinical PARP Inhibitors**. Cancer Res. (2012), Volume 72, Issue 21: 5588-99.

29. Tutt A, Robson M, Garber JE , et al**.: Oral poly(ADP-ribose) polymerase inhibitor olaparib in patients with BRCA1 or BRCA2 mutations and advanced breast cancer: A proof-of-concept trial**. The Lancet (2010), Volume 376: 235– 244.

30. O'Shaughnessy J, Osborne C, Pippen JE, et al. **Iniparib plus Chemotherapy in Metastatic Triple-Negative Breast Cancer**. N Engl J Med (2011), Volume 364: 205-214.

31. Konstantinopoulos PA, Wilson AJ, Saskowski J, et al. **Suberoylanilide hydroxamic acid (SAHA) enhances olaparib activity by targeting homologous recombination DNA repair in ovarian cancer**. Gynecol Oncol. (2014), Volume 133, Issue 3: 599–606.

32. Drugs.com, last updated 21 May 2020, <https://www.drugs.com/history/lynparza.html>.

33. Martin GM, Smith AC, Ketterer DJ, Ogburn CE, Disteche CM, Isr J. **Increased chromosomal aberrations in first metaphases of cells isolated from the kidneys of aged mice**. Med Sci. (1985), Volume 21, Issue 3: 296-301.

34. Chance B, Sies H, Boveris A. **Hydroperoxide metabolism in mammalian organs**. Physiol Rev. (1979), Volume 59, Issue 3: 527-605.

35. Friedberg EC, Walker GC, Siede W, Wood RD, Schultz RA, Ellenberger T. **DNA Repair and Mutagenesis**. ASM Press (2006): 1118.

36. Adachi N, Suzuki H, Iiizumi S, Koyama H. **Hypersensitivity of nonhomologous DNA end-joining mutants to VP-16 and ICRF-193: implications for the repair of topoisomerase II-mediated DNA damage**. J Biol Chem. (2003), Volume 278, Issue 38: 35897-902.

37. Sonoda E, Hochegger H, Saberi A, Taniguchi Y, Takeda S. **Differential usage of non-homologous end-joining and homologous recombination in double strand break repair**. DNA Repair (Amst). (2006), Volume 5, Issues 9-10: 1021-9.

38. Featherstone C, Jackson SP. **DNA double-strand break repair**. Current Biology (1999), Volume 9, Issue 20: 759-761.

39. Falzon M, Fewell JW, Kuff EL. **EBP-80, a transcription factor closely resembling the human autoantigen Ku, recognizes single- to double-strand transitions in DNA**. J Biol Chem. (1993), Volume 268, Issue 14: 10546-52.

40. Lieber MR. **The mechanism of human nonhomologous DNA end joining**. J Biol Chem. (2008), Volume 283, Issue 1: 1-5.

41. Niewolik D, Pannicke U, Lu H, Ma Y, Wang LC, Kulesza P, Zandi E, Lieber MR, Schwarz K. **DNA-PKcs Dependence of Artemis Endonucleolytic Activity, Differences between Hairpins and 5′ or 3′ Overhangs**. J. Biol. Chem. (2006), Volume 281: 33900–33909.

42. Daley JM, Palmbos PL, Wu D, Wilson TE. **Nonhomologous end joining in yeast**. Annual Review of Genetics (2005), Volume 39: 431–451.

43. Ma Y, Lu H, Tippin B, Goodman MF, Shimazaki N, Koiwai O, Hsieh CL, Schwarz K, Lieber MR. **A biochemically defined system for mammalian nonhomologous DNA end joining**. Mol. Cell (2004), Volume 16: 701–713.

44. Xuan L, Wolf-Dietrich H. **Homologous recombination in DNA repair and DNA damage tolerance**. Cell Res. (2008), Volume 18, Issue 1: 99–113.

45. Wold MS. **Replication protein A: a heterotrimeric, single-stranded DNA-binding protein required for eukaryotic DNA metabolism**. Annu Rev Biochem. (1997), Volume 66: 61-92.

46. Eggler AL, Inman RB, Cox MM. **The Rad51-dependent pairing of long DNA substrates is stabilized by replication protein A**. J Biol Chem. (2002), Volume 277, Issue 42: 39280-39288.

47. Kennedy RD, D'Andrea AD. **The Fanconi Anemia/BRCA pathway: new faces in the crowd**. Genes Dev. (2005), Volume 19, Issue 24: 2925-40.

48. Wong, A. K. C., Pero, R., Ormonde, P. A., Tavtigian, S. V. & Bartel, P. L. **RAD51 interacts with the evolutionarily conserved BRC motifs in the human breast cancer susceptibility gene brca2**. J. Biol. Chem. (1997), Volume 272: 31941–31944.

49. Yang H, Jeffrey PD, Miller J, Kinnucan E, Sun Y, Thoma NH, Zheng N, Chen PL, Lee WH, Pavletich NP. **BRCA2 function in DNA binding and recombination from a BRCA2–DSS1-ssDNA structure**. Science (2002), Volume 297: 1837-1848.

50. Bignell, G., Micklem, G., Stratton, M. R., Ashworth, A. & Wooster, R. **The BRC repeats are conserved in mammalian BRCA2 proteins**. Hum. Mol. Genet. (1997), Volume 6: 53–58.

51. Wong, A. K. C., Pero, R., Ormonde, P. A., Tavtigian, S. V. & Bartel, P. L. **Rad51 interacts with the evolutionarily conserved BRC motifs in the human breast cancer susceptibility gene brca2**. J. Biol. Chem. (1997), Volume 272: 31941–31944.

52. Pellegrini L, Yu DS, Lo T, Anand S, Lee M, Blundell TL, Venkitaraman AR. **Insights into DNA recombination from the structure of Rad51-BRCA2 Complex**. Nature (2002), Volume 420: 287–293.

53. Carreira A, Kowalczykowsky SC. **Two classes of BRC repeats in BRCA2 promote RAD51 nucleoprotein filament function by distinct mechanisms**. PNAS (2011), Volume 108, Issue 26: 10448-10453.

54. Shinohara, A., Ogawa, H. & Ogawa, T. **Rad51 protein involved in repair and recombination in S. cerevisiae is a RecA-like protein**. Cell (1992), Volume 69: 457–470.

55. West, S.C. **Molecular views of recombination proteins and their control**. Nat. Rev. Mol. Cell. Biol. (2003), Volume 4: 435–445.

56. Shin, D.S. et al. **Full-length archaeal Rad51 structure and mutants: mechanisms for Rad51 assembly and control by BRCA2**. EMBO J. (2003), Volume 22: 4566–4576.

57. Aihara, H., Ito, Y., Kurumizaka, H., Yokoyama, S. & Shibata, T. **The N-terminal domain of the human Rad51 protein binds DNA: structure and a DNA binding surface as revealed by NMR**. J. Mol. Biol. (1999), Volume 290: 495–504.

58. Yu, X., Jacobs, S.A., West, S.C., Ogawa, T. & Egelman, E.H. **Domain structure and dynamics in the helical filaments formed by RecA and Rad51 on DNA**. Proc. Natl. Acad. Sci. USA (2001), Volume 98: 8419–8424.

59. Bagnolini G, Milano D, Manerba M, Schipani F et al. **Synthetic Lethality in Pancreatic Cancer: Discovery of a New RAD51-BRCA2 Small Molecule Disruptor That Inhibits Homologous Recombination and Synergizes with Olaparib**. J. Med. Chem. (2020), Volume 63: 2588−2619.

60. Pellegrini L, Yu DS, Lo T, Anand S, Lee MY, Blundell TL, Venkitaraman AR. **Insights into DNA recombination from the structure of a RAD51–BRCA2 complex**. Nature (2002), volume 420: 287–293.

61. Seyfried TN, Flores RE, Poff AM, D'Agostino DP. **Cancer as a metabolic disease: implication for novel therapeutics**. Carcinogenesis (2014), Volume 35: 515-527.

62. Hanahan D, Weinberg RA. **Hallmarks of Cancer: The Next Generation**. Cell (2011), Volume 144, Issue 5: 646-674.

63. House SW, Warburg O, Burk D, Schade AL. **On Respiratory Impairment in Cancer Cells**. Science (1956), New Series, Vol. 124: 267-272.

64. Kroemer G, Pouyssegur J. **Tumor Cell Metabolism: Cancer's Achilles' Heel**. Cancer Cell (2008), Volume 13, Issue 6: 472-482.

65. DeBerardinis RJ, Lum JJ, Hatzivassiliou G, Thompson CB. **The Biology of Cancer: Metabolic Reprogramming Fuels Cell Growth and Proliferation**. Cell Metabolism (2008), Volume 7, Issue 1: 11-20.

66. Kato Y, Ozawa S, Miyamoto C, Maehata Y, Suzuki A, Maeda T, Baba Y. **Acidic extracellular microenvironment and cancer**. Cancer Cell International (2013), Volume 13, Article number: 89.

67. Yabu M, Shime H, Hara H, Saito T, Matsumoto M, Seya T, Akazawa T, Inoue N. **IL-23-dependent and -independent enhancement pathways of IL-17A production by lactic acid**. Int Immunol. (2011), Volume 23, Issue 1: 29-41.

68. Matsuura K, Canfield K, Feng W, Kurokawa M. **Metabolic Regulation of Apoptosis in Cancer**. Int Rev Cell Mol Biol. (2016), Volume 327: 43–87.

69. Jia D et al. **Elucidating cancer metabolic plasticity by coupling gene regulation with metabolic pathways**. Proc Natl Acad Sci USA (2019), Volume 116: 3909–3918.

70. Semenza GL et al. **Hypoxia response elements in the aldolase A, enolase 1, and lactate dehydrogenase A gene promoters contain essential binding sites for hypoxia-inducible factor 1**. J Biol Chem (1996), Volume 271: 32529–32537.

71. McFate T, Mohyeldin A, Lu H, Thakar J et al. **Pyruvate Dehydrogenase Complex Activity Controls Metabolic and Malignant Phenotype in Cancer Cells**. The Journal of Biological Chemistry (2008), Volume 283: 22700 –22708.

72. Semenza GL. **Defining the role of hypoxia-inducible factor 1 in cancer biology and therapeutics**. Oncogene (2010), Volume 29: 625–634.

73. Markert CL, Shaklee JB and Whitt GS. **Evolution of a Gene**. Science (1975), New Series, Volume 189: 102-114.

74. Shim H, Dolde C, Lewis BC, et al. **c-Myc transactivation of LDH-A: Implications for tumor metabolism and growth**. Proc. Natl. Acad. Sci. USA (1997), Volume 94: 6658–6663.

75. Rani R, Kumar V. **Recent update on human lactate dehydrogenase enzyme 5 (hLDH5)**
inhibitors: a promising approach for cancer chemotherapy. J. Med. Chem. (2016), Volume 59: 487- 496.

76. Goldberg E, Eddy EM, Duan C, Odet F. **LDHC THE ULTIMATE TESTIS SPECIFIC GENE**. J Androl. (2010), Volume 31, Issue 1: 86–94.

77. Read JA, Winter VJ, Eszes CM, Sessions RB, Brady RL. **Structural basis for altered activity of M- and H-isozyme forms of human lactate dehydrogenase**. Proteins (2001), Volume 43, Issue 2: 175-185.

78. A.E. Boukouris, S.D. Zervopoulos, E.D. Michelakis. **Metabolic enzymes moonlighting in the nucleus: metabolic regulation of gene transcription**. Trends Biochem. Sci. (2016), Volume 41: 712-730.

79. R.P. Dai, F.X. Yu, S.R. Goh, H.W. Chng, Y.L. Tan, J.L. Fu, L. Zheng, Y. Luo. **Histone 2B (H2B) expression is confined to a proper NAD+/NADH redox status**. J Biol Chem (2008), Volume 283: 26894-26901.

80. Zhong XH, Howard BD. **Phosphotyrosine-containing lactate dehydrogenase is restricted to the nuclei of PC12 pheochromocytoma cells**. Molecular and Cellular Biology (1990), Volume 10: 770-776.

81. Fiume L, Manerba M, Vettraino M, Di Stefano G. **Inhibition of lactate dehydrogenase activity as an approach to cancer therapy**. Future Med. Chem. (2014), Volume 6: 429-445.

82. Sheng SL, Liu JJ, Dai YH, Sun XG, Xiong XP, Huang G. **Knockdown of lactate dehydrogenase A suppresses tumor growth and metastasis of human hepatocellular carcinoma**. FEBS J (2012), Volume 279: 3898–910.

83. Zhai X, Yang Y, Wan J, Zhu R, Wu Y. **Inhibition of LDH-A by oxamate induces G2/M arrest, apoptosis and increases radiosensitivity in nasopharyngeal carcinoma cells**. Oncology Reports (2013), Volume 30, Issue 6: 2983-2991.

84. Yeung C, Gibson AE, Issaq SH, et al. **Targeting Glycolysis through Inhibition of Lactate Dehydrogenase Impairs Tumor Growth in Preclinical Models of Ewing Sarcoma**. Cancer research (2019), Volume 79, Issue 19: 5060-5073.

85. Bhatt AN, Chauhan A, Khanna S, Rai Y, Singh S, Soni R, Kalra N, Dwarakanath BS. **Transient elevation of glycolysis confers radio-resistance by facilitating DNA repair in cells**. BMC Cancer (2015), Volume 15: 335.

86. M.A.T. vanVugt. **Shutting down the power supply for DNA repair in cancer cells**. J. Cell Biol. (2017), Volume 216: 295-297.

87. Latham T, Mackay L, Sproul D, Karim M, et al. **Lactate, a product of glycolytic metabolism, inhibits histone deacetylase activity and promotes changes in gene expression**. Nucleic Acids Research (2012), Volume 40, Issue 11: 4794–4803.

88. Zhang D, Tang Z, Huang H, Zhou G, et al. **Metabolic regulation of gene expression by histone lactylation**. Nature (2019), Volume 574: 575–580.

89. Dos Santos Ferreira AC, Fernandes RA, Kwee JK, Klumb CE. **Histone deacetylase inhibitor potentiates chemotherapy-induced apoptosis through Bim upregulation in Burkitt's lymphoma cells**. Journal of Cancer Research and Clinical Oncology (2012), Volume 138: 317–325.